The Date of Appearance of Philistine Pottery at Megiddo: A Computational Approach

Eythan Levy, Israel Finkelstein, Mario A. S. Martin, and Eli Piasetzky

This paper addresses the question of the date of appearance of Philistine Bichrome pottery at Megiddo through a new computational approach, using recently developed chronology software. Based on historical dates, we obtain a terminus post quem of 1183 B.C.E. for the start of Philistine Bichrome at Megiddo using a broad model, and a terminus post quem of 1124 B.C.E. under stronger chronological hypotheses. Adding radiocarbon results at 68.2% confidence level to the model yields a narrow range of 1111–1086 B.C.E. for the appearance of Bichrome (1128—1079 B.C.E. for 95.4%). The paper also presents results suggesting that Stratum VIIB ended during, or only slightly before, the reign of Ramesses III (1184–1153 B.C.E.).

This paper deals with the question of the date of appearance of Philistine Bichrome pottery at Megiddo (northern Israel) using a computational approach. The chronology of the early Philistine settlement is of significant historical importance for the Late Bronze/Iron I transition (see Ben-Dor Evian 2017; for an overview of current developments in the history of the Philistines and other Sea Peoples, see Kahn 2011). Over 20 years ago, Finkelstein (1995, following Ussishkin 1985) introduced the Low Philistine Chronology, proposing that the arrival of the Philistines on the south Levantine coast should be dated no earlier than the later days of Ramesses VI (1143–1136). He thus challenged the then-consensual, so-called "Middle Chronology," which set their arrival during the 8th year of Ramesses III (1177 B.C.E.). The debate on the absolute dating of the Philistine settlement thus rages to this day, now adding radiocarbon results to ceramic and textual considerations. Recent papers have defended both an ultra-high Philistine chronology (Asscher, Cabanes et al. 2015; Asscher, Lehmann et al. 2015; see also Asscher and Boaretto 2019) and a low one (Finkelstein 2016, 2018). Another recent development (Finkelstein et al. 2017) focused on dating the appearance of Philistine pottery in the northern site of Megiddo, outside of Philistia proper. This study fixed the appearance of Bichrome pottery at Megiddo in the late 12th/early 11th century, based on radiocarbon results combined with a meticulous stratigraphic and ceramic investigation.

In this paper, we approach the question of the date of appearance of Philistine pottery at Megiddo differently, based on formal modeling of chronological constraints. This modeling was realized using ChronoLog, a chronological software application based on deterministic (i.e., non-statistical) algorithmic techniques (see Levy et al. 2021; chrono.ulb.be). This methodology (presented in detail below), allows researchers to encode a broad set of chronological constraints, including historical and stratigraphic sequences, termini post/ante quem, and diverse types of synchronisms. The software then checks the consistency of the encoded model and computes the tightest possible time-ranges for each start date, end date, and duration. The model can be interactively queried by adding/removing/updating data and immediately checking the effect of a given change on the overall chronology. The strength

Eythan Levy: Institute of Archaeology, Tel Aviv University, P. O. Box 39040, Tel Aviv 69978, Israel; *eythan.levy@gmail.com*

Israel Finkelstein: School of Archaeology and Maritime Cultures, University of Haifa, Mount Carmel, Haifa, 3498838; Institute of Archaeology, Tel Aviv University, P. O. Box 39040, Tel Aviv 69978, Israel; *fink2@tauex.tau.ac.il*

Mario A. S. Martin: Institute of Archaeology, Tel Aviv University, P. O. Box 39040, Tel Aviv 69978, Israel; Leon Recanati Institute for Maritime Studies, University of Haifa (RIMS), Mount Carmel, Haifa, 3498838, Israel; *mario_antonio@outlook.com*

Eli Piasetzky: School of Physics and Astronomy, Tel Aviv University, Tel Aviv 69978, Israel; *eip@tauphy.tau.ac.il*

Electronically Published March 4, 2022.

Bulletin of ASOR, volume 387, May 2022. https://doi.org/10.1086/719048

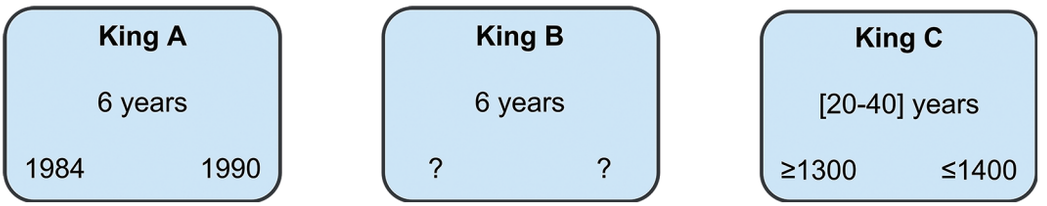

Fig. 1. Three examples of periods: King A reigned for 6 years between 1984 and 1990, King B reigned for 6 years at an unknown date, and King C reigned between 20 and 40 years at some point between 1300 and 1400. (Chart by E. Levy)

of the computer-assisted approach lies in the fact that it enables the researcher to address large bodies of data, featuring hundreds of synchronisms, termini post/ante quem, and duration estimates—a feat impossible to achieve by manual treatment of the data. In such large models, the human brain is prone to miss relevant correlations between data and thus fails to obtain optimal chronological estimates. We do not profess that this computational approach yields ultimate, undisputable answers, as we are aware that these results depend on subjective input. But the fact that our models include large sets of data of diverse origins (Egyptological, radiometric, ceramic, stratigraphic) does tend to augment the robustness and reliability of the proposed results.

We illustrate this approach here for the first time on a large case study, involving the reign of several Egyptian pharaohs, stratigraphic sequences, radiocarbon results, and archaeological periods. More precisely, we are interested in obtaining computer-generated termini post/ante quem results for the start of Bichrome pottery at Megiddo, under diverse sets of hypotheses regarding radiocarbon results and Egyptian synchronisms. Our results, methodology, and data are presented below.

Methodology

This section presents an overview of the ChronoLog methodology (see Levy et al. 2021 for full details).

Definitions

ChronoLog models are based on the following three types of data:

Period. A *period* represents a continuous interval of time. It is characterized by a start date, an end date, and a duration. These can bear the following types of chronological constraints: a start or end date can be unknown, known (e.g., 1984 C.E.), lower bounded (after 1984 C.E.), upper bounded (before 1984 C.E.), or in a range (e.g., between 1984 and 1990 C.E.). In the same way, durations can also be unknown, known (e.g., 5 years), lower bounded (at least 5 years), upper bounded (at most 5 years) or in a range (e.g., between 5 and 10 years). A period is thus represented by six numbers at most: minimum duration, maximum duration, earliest start date, latest start date, earliest end date, and latest end date.

Sequence. A *sequence* represents a set of consecutive periods, with no gaps between them.[1] Hence, the end date of a period always equals the start date of the next period in the sequence.

Synchronism. A *synchronism* represents a chronological relationship between two periods. ChronoLog supports many types of synchronisms, three of which are used in this paper:

Contemporaneity. This is the most common type of synchronism, representing two periods having at least one day in common.[2]

Synchronized Transition. The start or end of a given period equals the start or end of another period.

Ordered Transition. The start or end of a given period is earlier/later than the start or end of another period.[3]

For more details on ChronoLog synchronisms, see Levy et al. 2021: 2–6 and Levy, Piasetzky, and Fantalkin 2021.

The date/duration constraints and synchronisms of a ChronoLog model constitute a set of *input* data that the software will use in order to compute the final chronology (see "Functionalities of the Software" below).

Graphical Notations

Period. A period is represented by a rectangle with its name on top, its duration in the middle, its start date at the bottom left corner, and its end date at the bottom right corner. Ranges are represented with square brackets (e.g., "1984–1990"), upper bounds with the "≤" sign ("≤ 1984"), lower bounds with the "≥" sign ("≥ 1984"), and unknown dates or duration with a question mark (example in **Fig. 1**).

[1] A gap between two periods can also be represented as a period.

[2] A contemporaneity synchronism between periods A and B is formalized as "end(A) ≥ start(B) and end(B) ≥ start(A)" (see, for example, Holst 2004: 138 and Geeraerts, Levy, and Pluquet 2017: 7). Note that ChronoLog uses year-precision.

[3] In this case, we use non-strict inequalities, that is, "after" means "after or at," and "before" means "before or at."

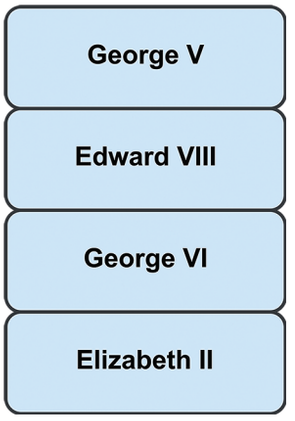

Fig. 2. An example of a sequence (Windsor Dynasty, with dates and durations omitted). (Chart by E. Levy)

Sequence. A sequence is represented by vertically stacking consecutive periods, from the earliest to the latest (**Fig. 2**).

Synchronism. Three types of synchronisms are used in this paper (see **Fig. 3**):

Contemporaneity. A line connecting two rectangles at the center of the short side of the rectangle (**Fig. 3**, left).

Synchronized Transition. A line connecting the corners of two rectangles (**Fig. 3**, center).

Ordered Transition. An arrow connecting the corners of two rectangles, from the earliest to the latest start/end date (**Fig. 3**, right).

Expressiveness of the Model

The ChronoLog data model allows expression of most of the useful chronological relations relevant to archaeology (see Levy et al. 2021: 2–6). Periods can contain termini post/ante quem and duration estimates, thus enabling the modeling of both floating sequences and sequences having absolute dates. Sequences can represent archaeological layers, dynasties, and ceramic families (including gaps and overlaps, represented by periods of their own). Synchronisms can be used to model all sorts of correlations between monarchs, layers, and archaeological periods.

Functionalities of the Software

ChronoLog has three main functionalities:

Chronological Computation. Once a ChronoLog model is encoded, the software computes the optimal (i.e., tightest possible) range for each start date, end date, and duration. These optimal ranges are obtained by combining the period's encoded data (range or terminus post/ante quem) with data originating from other periods through the use of synchronisms. If the data in the model are contradictory, the software will detect and report the contradiction. Furthermore, for each computed range (or contradiction result), the software provides a full justification of the result, expressed as a path in the chronological network, combining synchronisms with date/duration constraints (see examples in "Results" below). The chronological computation is based on efficient graph-theoretic algorithms (see Geeraerts, Levy, and Pluquet 2017; Levy et al. 2021: 11–16). These algorithms produce *deterministic* (i.e., non-probabilistic) ranges, meaning these ranges are not associated with a given probability: they are certain, provided the given inputs are correct. They are also extremely fast: the models presented in this paper ran in less than one second each, on a simple personal computer.

Testing Hypotheses. The ChronoLog algorithms enable interactive use of the software in order to test specific hypotheses. More specifically, the researcher can update/add/remove any date, duration, or synchronism and immediately see its chronological impact on the model, as the optimal ranges are re-calculated on the fly. In other words, ChronoLog allows us to immediately assess the global impact of local chronology-related changes. When such a local change is introduced, three outcomes are possible: a) a *contradiction* is detected, meaning that the update is incompatible with the other data of the model; b) the update is *neutral*, meaning no contradiction is detected, but the update yields no change to any other date or duration in the model; or c) the update is *effective*, meaning it does have an impact on the model, and at least one date or duration gets modified.

Selective Chronologies. One particular type of hypothesis testing is the automatic generation of selective

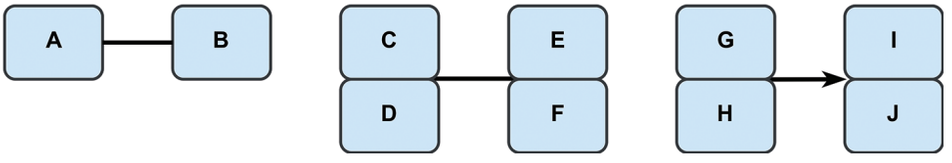

Fig. 3. Three examples of synchronisms: A is contemporaneous with B, C ends at the same time as E (synchronized transition), G ends before the start of J (ordered transition). (Chart by E. Levy)

chronologies. Data in ChronoLog is *tagged*—each sequence is associated with a list of tags (keywords), such as "radiocarbon," "stratigraphy," "Egypt," etc. ChronoLog allows researchers to interactively select/unselect tags in order to include the associated data in the model or exclude them from it. When dealing with a large model involving historical, stratigraphic, ceramic, and radiocarbon data, this enables users to immediately obtain alternative chronologies based on the exclusion of one or several types of data, thus helping researchers to answer questions such as: "what does the chronology become if all ceramic data are excluded?" This important feature allows researchers to obtain *several* different chronologies for a problem at hand (called here "selective chronologies") instead of just one, and to attain them *automatically* through the software, with little effort other than the encoding of the basic underlying data.

Advantages of Our Approach

The ChronoLog approach presents several advantages:

Rigor. The algorithmic computation of dates provided by ChronoLog offers greater rigor than manually-assessed chronological results, which are more cumbersome to obtain and error-prone, especially for large models.

Optimality. For a given set of chronological hypotheses, ChronoLog provides the tightest possible ranges for each start date, end date, and duration (see Levy et al. 2021: 6–7).

Clear Disclosure of Hypotheses. The ChronoLog approach forces researchers to *explicitly* lay down all the ground hypotheses on which the final chronology will rely. This transparency aspect adds rigor and scientific credence to the final published chronological results.

Related Works

Our work lies in the field of mathematical modeling of chronological constraints. Most current work in this field is of a probabilistic nature. The best-known approach is Bayesian modeling of radiocarbon dates, where chronological constraints (called "priors") are inserted into the radiocarbon calibration process, in order to obtain more precise confidence intervals (Buck et al. 1991; Bronk Ramsey 2009; see also "Radiocarbon Dating" below). More recent probabilistic approaches combine Bayesian modeling, Monte-Carlo simulation, and summed probability distribution of radiocarbon dates (Crema and Kobayashi 2020). Other probabilistic techniques recently applied to chronological modeling include aoristic analysis (Johnson 2004; Crema 2012) and evidence density estimation (Demján and Dreslerová 2016). The ChronoLog methodology, however, is based on a deterministic (i.e., non-probabilistic) approach. It models chronological uncertainty on dates and durations by *ranges*, rather than probability distributions. These ranges are then tightened as much as possible, by combining the information provided by all the input constraints. A similar deterministic approach was followed by Bruno Desachy (2016), whose tool, *Chronophage*,[4] reduces the span of chronological ranges in archaeological stratigraphy, though using a more restricted data model and different algorithms than ours. Another deterministic approach is that of Alfred Kromholz (1987), whose pioneering work showed how standard business-oriented software can be used to build archaeological chronologies using the so-called "critical path method." Finally, David Falk developed a deterministic tool, *Groundhog*,[5] for testing the validity of historical chronologies given a set of dynastic sequences and synchronisms (Falk 2016, 2020). *Groundhog* uses a different data model than ChronoLog, and relies on exhaustive search, while ChronoLog uses a faster approach, based on shortest path algorithms.

About ChronoLog

ChronoLog rests on mathematical foundations inspired from the fields of temporal logics and graph theory. The set of chronological constraints in the model is encoded as one long logical formula, which is then translated into a graph (a mathematical object representing a network of related items). The computation of the optimal ranges is then done by computing shortest paths in this graph, like a navigation application, but finding here shortest paths in time rather than in space. A general description of ChronoLog can be found in Levy et al. 2021. A technical description of the mathematics and algorithms behind ChronoLog can be found in Geeraerts, Levy, and Pluquet 2017. For the use of ChronoLog as a cross-dating tool, see Levy, Piasetzky, and Fantalkin 2021. ChronoLog is available online (chrono.ulb.be) and can be downloaded at no cost.

Megiddo: Data and Modeling Rules

Our models for the appearance of Philistine Bichrome pottery at Megiddo include five types of data: (1) stratigraphic sequences, (2) archaeological periods, (3) stratified dateable Egyptian artifacts, (4) stratified Bichrome pottery, and (5) radiocarbon dating. Each one of them is presented below, including methodological modeling guidelines.

Stratigraphy

Our models include three stratigraphic sequences from Megiddo, namely the University of Chicago excavations

[4] *Chronophage* is available online at https://abp.hypotheses.org/4284.
[5] See http://www.groundhogchronology.com.

strata-system and the Areas K and H levels of the renewed Tel Aviv University (TAU) excavations. The modeled layers (Chicago IX to IVA, TAU K-9 to K-1 and H-15 to H-3) cover the period from Late Bronze (LB) I to the end of Iron IIB. The following additional sets of input data have been added to our models:

Duration Estimates. For each layer, a broad duration estimate has been added, provided by the current Megiddo excavators, on the basis of elements such as architectural changes, raising of floors, and thickness of occupational accumulation. The durations are given as ranges and fall into four categories: short (10–50 years), medium-short (25–100 years), medium-long (50–100 years), and long (50–150 years). In each case, a maximalist approach has been followed, as a stratum estimated by the excavators to be 40–50 years long was typically assigned a cautious 25–100-year duration range (medium-long).[6]

End Dates for the Sequences. An absolute date of 732 B.C.E. (unanimously agreed upon concerning the takeover of Megiddo by Assyria) was imposed on the last Iron IIB layer[7] in each sequence (Strata IVA, Levels K-2 and H-5).

Synchronized Destructions. Synchronisms have been added in order to represent layers considered by the excavators as having been destroyed (or disrupted) at the same time. These synchronisms concern the following layers: Level K-8 synchronized with Stratum VIIB, Level H-11 with Stratum VIIA, Levels K-4 and H-9 with Stratum VIA, and Level K-2 with H-5 (see Finkelstein et al. 2017: 269, 275, 277, with reference to previous and in press works).

Gap Periods. A period of 0 to 40 years duration has been inserted after each destruction layer, representing a possible gap before the start of the next period. Such gap periods have been inserted after Strata VIIA, VIA, and VA-IVB, and Levels K-6, K-4, K-2, H-9, and H-5.

Our stratigraphic data are summarized in **Figure 4**.

Archaeological Periods

We will now add to our models the local sequence of archaeological periods as defined by ceramic typology. This sequence ranges from LB I to Iron IIB, including LB IIA, LB IIB, LB III, early Iron I, late Iron I, early Iron IIA, and late Iron IIA. The sequence is left floating (i.e., not featuring any absolute dates). Duration estimates are, however, added for each period, using sufficiently broad ranges as to be consensual among the diverse current south Levantine chronologies (see **Fig. 5**). We will then add correlations between layers of different areas, according to their ceramic typology. We will finally also add synchronisms representing the presence/absence of specific pottery types from our layers, using the set of rules defined hereunder.

Modeling Rules. Two types of synchronisms between layers and archaeological periods will be used: presence and absence of specific ceramic types in a given layer.

Contemporaneity Synchronisms. Whenever two layers (in different areas, say A-3 and B-7) feature the same pottery type (say LB I), a common methodological mistake is to posit a contemporaneity synchronism between them. This is not correct, since A-3 and B-7 could have similar pottery and yet not be contemporaneous (e.g., A-3 could be early LB I, and B-7 late LB I).[8] The correct way to model such cases is to add contemporaneity synchronisms between the layers and the associated archaeological period, and no direct synchronisms between the layers themselves. In our example, we would thus have one contemporaneity synchronism between Layer A-3 and LB I, and another one between Layer B-7 and LB I, rather than a direct A-3–B-7 synchronism.

Ordered Transitions. When the excavator is certain about the absence of a given pottery type from a given layer, he/she may wish to model the fact that this layer pre- or postdates specific archaeological periods. This will be modeled through "ordered transition" synchronisms (see "Definitions" above). More precisely, for each layer, two such synchronisms will be added: one representing the absence of early ceramic types and another representing the absence of late pottery types from the layer. For example, if Layer A-2 is considered to be wholly included within the LB IIA, the following two ordered transition synchronisms would be added: A-2 starts

[6] The duration ranges for archaeological strata can only be estimated with large uncertainties. In some cases, elements such as architectural changes, raising of floors, and thickness of occupational accumulation can indeed provide a rough indication as to whether a stratum was short or long-lived, but even then, much is left to the excavator's subjective assessment. In such cases, broad ranges should be used. For example, in the Megiddo case, the famous "Solomonic" stratum VA–IVB has been assigned durations of 60 years by Aharon Kempinski (1989, p. 10) and 70 years by Ussishkin (2018, p. 15). In our model, we assign it a wide range of 50–150 years. Once assigned, sensitivity to the given ranges should be checked. In many cases, only a few duration estimates are really critical. For example, in the Historical Model presented below, the earliest start of the Philistine Bichrome relied on only three duration bounds (Strata VIIA, K-6, and K-7).

[7] Throughout the article, we use "stratum" for the Megiddo layers excavated by the University of Chicago and "level" for those excavated by Tel Aviv University. We use the neutral word "layer" when not referring to a specific excavation.

[8] In mathematical terms, the contemporaneity relationship is not transitive.

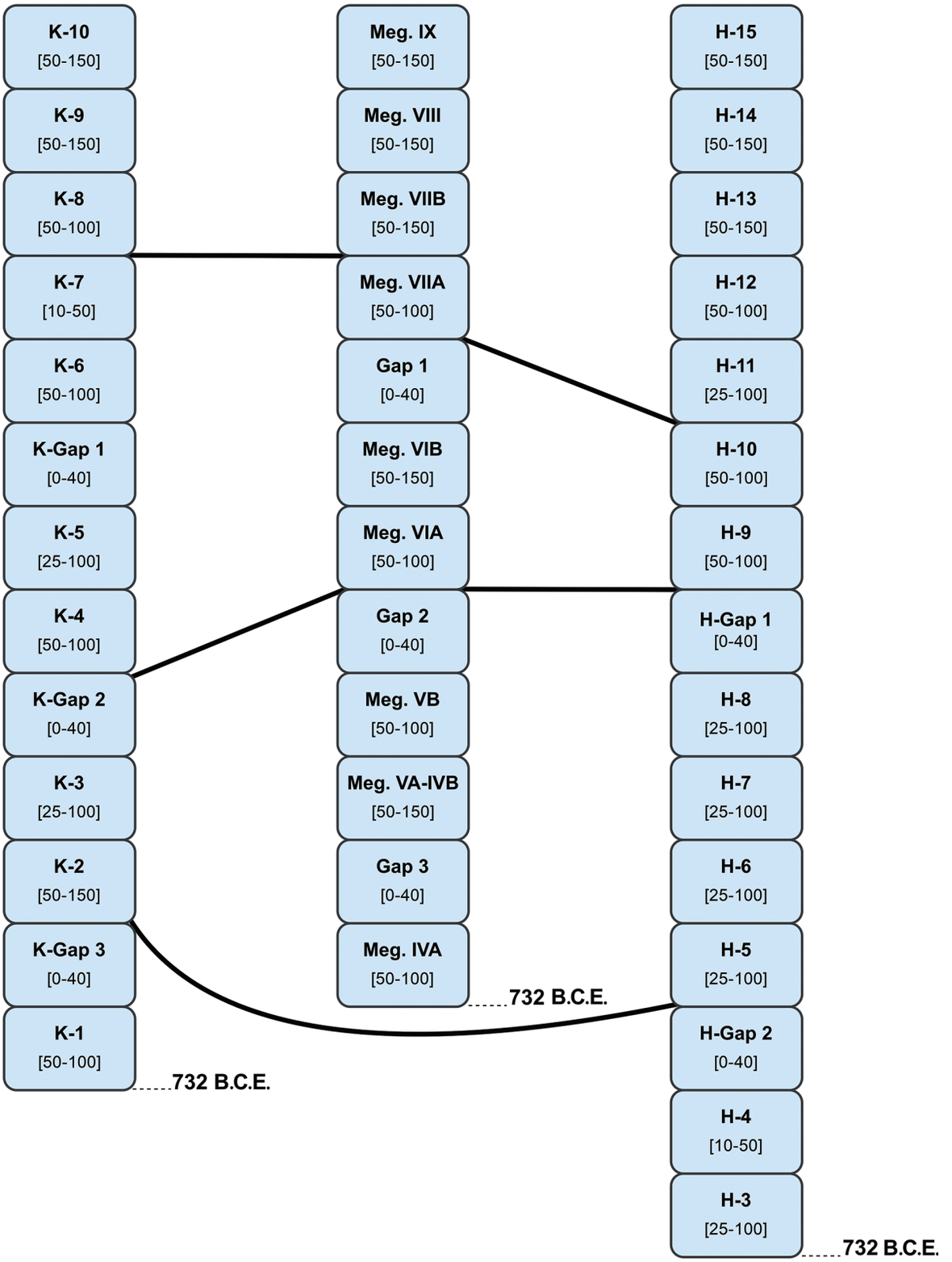

Fig. 4. Stratigraphic sequences used in our models, featuring duration estimates, a 732 B.C.E. ending for all three sequences, and synchronized endings between layers. Each stratum ending by destruction is followed by a gap period. (Chart by E. Levy)

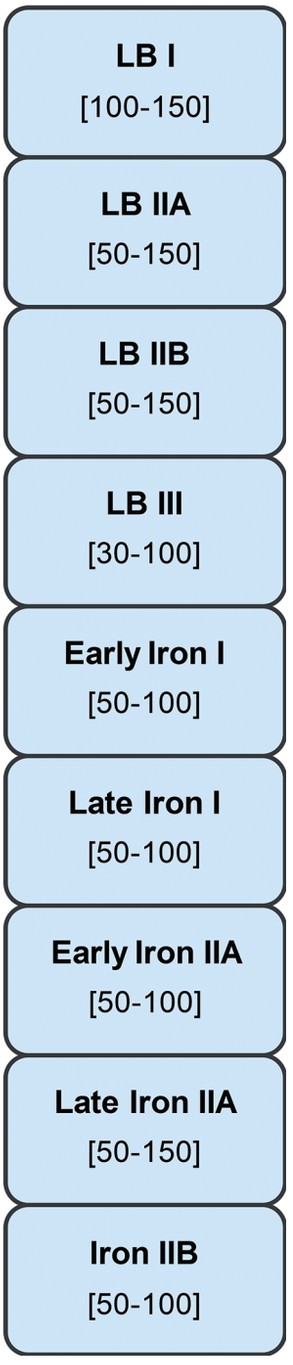

Fig. 5. Sequence of archaeological periods used in this paper, from the Late Bronze I to the Iron IIB, with broad duration estimates for each period. (Chart by E. Levy)

after the end of Late LB I, and A-2 ends before the start of LB IIB.

Data. Let us now add synchronisms between the archaeological periods and our layers, following the modeling rules defined above. These synchronisms (provided by the site excavators) are presented in **Figure 6** (contemporaneity synchronisms) and **Figure 7** (ordered transitions). The full list of these synchronisms is also presented in **Appendix A**.

Egyptian Synchronisms

This section presents stratified datable Egyptian material found at the site that enables us to add synchronisms between historically dated Egyptian pharaohs and specific layers. It will thus provide us with sources of absolute dating for our stratigraphic sequences. These synchronisms will be added using the modeling rules presented hereunder. As for absolute chronology, we use Kenneth Kitchen's standard dates for the 18th, 19th and 20th Egyptian dynasties[9] (2000, see **Table 1**).[10] These dynastic dates will provide the backbone for absolute chronology in our first (non-radiocarbon-based) model (see "Results" below).

Modeling Rules. The following set of rules enables us to add safe synchronisms between layers and datable artifacts (see Levy, Piasetzky, and Finkelstein 2020: 4):

Rule 1 (Basic Rule). An artifact of King K found in Layer L is formalized as "Layer L ends after the start of King K's reign."

This rule maintains that the *start* of the reign provides a terminus post quem (TPQ) for the *end* of the layer. In other words, a layer cannot end before the accession date of a king whose artifact was found in it. Note that since the rule uses only a TPQ (rather than a contemporaneity synchronism), it also holds if the artifact is an heirloom or if it was manufactured after King K's death. We now extend Rule 1 to cases of uncertain reign:

Rule 2 (Uncertain Reign). An artifact of unknown reign, but having King K as *earliest possible reign*, found in Layer L, is formalized as "Layer L ends after the start of King K's reign."

Rule 2 is useful in particular for scarabs only datable to a specific dynasty, part of a dynasty or when the royal name is only partly legible, making the identification of the king equivocal. Rule 1 can also be extended to cases of uncertain layer:

Rule 3 (Uncertain Layer). An artifact of King K found in an unknown layer, but with Layer L as the *latest possible layer*, is formalized as "Layer L ends after the start of King K's reign."

[9] Egyptian finds earlier than the 18th Dynasty, though existing at Megiddo, were not included in our models, as we restrict ourselves to the Late Bronze and Iron Ages. Note also that finds later than the 20th Dynasty are absent from the table, although Third Intermediate Period scarabs are known at Megiddo, yet from unclean contexts (see nn. 16–17 below).

[10] See Schneider 2010 for a higher alternative.

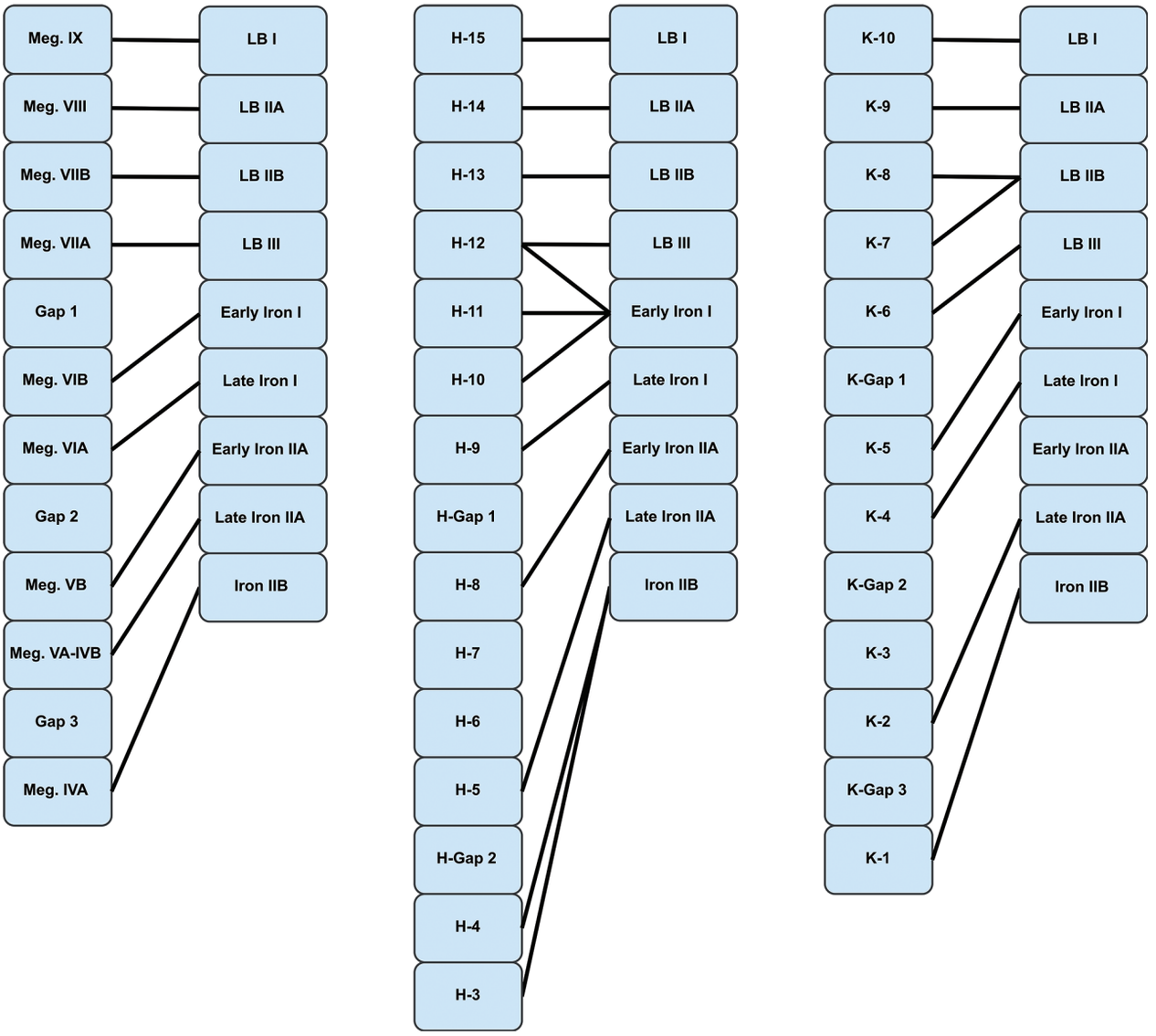

Fig. 6. Contemporaneity synchronisms between layers and archaeological periods, based on ceramic evidence. No synchronism is added for Levels H-6, H-7, and K-3 because the pottery assemblages from these layers were not clear enough to allow differentiating between early and late Iron IIA. (Chart by E. Levy)

Rule 3 is handy for cases where the excavator hesitates between several layers for his artifact (as for scarabs found under the floor of a house). Finally, the rule can be extended to cases of uncertain reign and layer:

Rule 4 (Uncertain Reign and Layer). An artifact of unknown reign but having King K as *earliest possible reign*, found in an unknown layer, but with Layer L as *latest possible layer*, is formalized as "Layer L ends after the start of King K's reign."

Note that these TPQ rules are much more cautious than modeling a simple contemporaneity synchronism between the artifact and its layer of discovery. Furthermore, as noted above for Rule 1, these TPQ even hold in cases of heirlooms or artifacts bearing the name of long-deceased kings. In summary, the above rules simply amount to building a TPQ that combines the latest possible layer with the earliest possible reign of the given monarch related to the artifact. They thus do not require the knowledge of an earliest possible layer nor of a latest possible reign for the artifact.

Data. The full corpus of Egyptian material included in our models is presented in **Table 2**, together with the synchronisms derived from the four rules defined above. The corpus includes the Ramesses VI statue base from

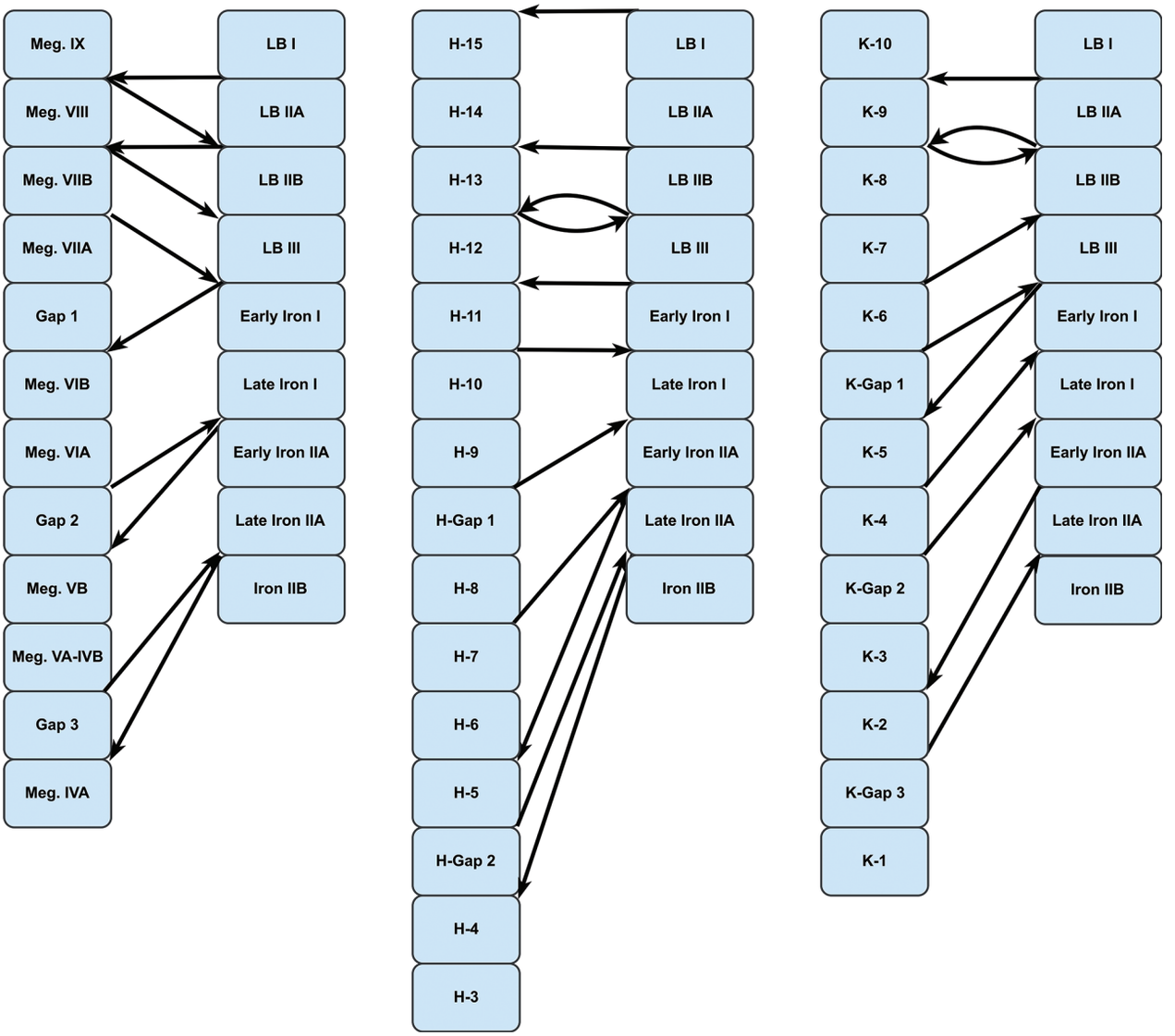

Fig. 7. Ordered transition synchronisms between layers and archaeological periods. An arrow between transitions A and B represents the "A is earlier or equal to B" relationship. All the "starts after the end of" synchronisms have been rewritten as "ends before start of" synchronisms for the sake of clarity, and redundant synchronisms have been removed from the figure for the sake of conciseness (see **Appendix A** for the full list of synchronisms). (Chart by E. Levy)

Stratum VIIA[11] (Breasted 1948), the Ramesses III ivory pen-case from Stratum VII (undivided)[12] (Loud 1939: 9–12), the datable[13] Area K and Area H scarabs from the current Tel Aviv University excavations,[14] and various datable scarabs from the old University of Chicago excavations.[15] Scarabs that were described in the reports as coming from

[11] The statue base was found buried beneath a Stratum VIIB wall in Area CC (Breasted 1948: 135, n. 1), but is assigned to Stratum VIIA (see discussion in Ussishkin 1995: 259–60).

[12] The Ramesses III pen-case is part of the ivory hoard found in the Stratum VIIA palace. The excavator expressed doubts as to whether these ivories belong to the timespan of Stratum VIIA or (all or some) were heirlooms from Stratum VIIB (Loud 1939: 9; see also the recent discussion in Martin 2017a: 273, 283).

[13] The scarabs discussed in this section are dated either by the presence of a royal name or stylistically.

[14] The Tel Aviv scarabs were gathered from the Tel Aviv excavation reports, covering the 1992–2014 seasons.

[15] The old Oriental Institute excavation reports did not provide a systematic analysis and dating of each scarab, hence part of our data comes from a review of secondary literature such as Bertha Porter and Rosalind Moss's *Topographical Bibliography* (1952: 380–81), the recent *Megiddo 3* volume by Tim Harrison (2004), Kempinski's (1989) monograph on Megiddo, and Baruch Brandl's (2004) assessment on 20th-Dynasty scarabs from Canaan.

unsecure loci,[16] or having unsecure Egyptian dating,[17] were discarded.

Optimality Issues. Our corpus includes Egyptian artifacts of unequal chronological value. For example, Stratum VIIA has two TPQs, one deriving from the Ramesses VI statue base and one from Ramesses III artifacts (pen-case and scarab). In this case, it is clearly the Ramesses VI statue base that provides the optimal (i.e., latest) TPQ for Stratum VIIA. Hence the Ramesses III artifacts could be considered as dispensable. Such "dispensable" artifacts are nevertheless included in our models, in order to enable us to perform hypothesis testing (see "Functionalities of the Software" above). Indeed, testing hypotheses by hiding/showing selected artifacts or updating selected synchronisms could change the status of a "dispensable" artifact, potentially enabling it to yield a new optimal TPQ. Such an experiment, in which the formerly "dispensable" Ramesses III pen-case now yields an optimal TPQ, will be presented in "Result 2" below.

Table 1. Absolute Chronology of the 18th, 19th, and 20th Egyptian Dynasties (Adapted from Kitchen 2000)

18th Dynasty	
Ahmose I	1540–1515
Amenhotep I	1515–1494
Thutmose I	1494–1482
Thutmose II	1482–1479
Hatshepsut	1479–1457
Thutmose III (sole reign)	1457–1425
Amenhotep II (sole reign)	1425–1401
Thutmose IV	1401–1391
Amenhotep III	1391–1353
Amenhotep IV	1353–1337
Smenkhare (sole reign)	1337–1336
Tutankhamun	1336–1327
Ay	1327–1323
Horemheb	1323–1295
19th Dynasty	
Ramesses I	1295–1294
Seti I	1294–1279
Ramesses II	1279–1213
Merneptah	1213–1203
Amenmesse	1203–1200
Seti II	1200–1194
Siptah	1194–1188
Twosret (sole reign)	1188–1186
20th Dynasty	
Sethnakhte	1186–1184
Ramesses III	1184–1153
Ramesses IV	1153–1147
Ramesses V	1147–1143
Ramesses VI	1143–1136
Ramesses VII–XI	1136–1070

Philistine Bichrome

In this section we model the presence of Philistine pottery in our three stratigraphic sequences (see Finkelstein et al. 2017 for a full discussion) using modeling rules similar to those defined above for archaeological periods. A new period is added to the model, representing the full timespan of Philistine pottery at Megiddo.[18] A broad and

[16] Scarabs discarded due to unsecure stratigraphic affiliation are the following:

1. Scarab 10/H/1/AR1 (Thutmose IV): found during cleaning (Ben-Dor Evian and Münger in press)
2. Scarab 10/H/30/AR5 (19th Dynasty): found in a pit (Ben-Dor Evian and Münger in press)
3. Scarab 06/K/118/AR1 (19th–20th Dynasty): baulk removal, "probably Level K-6" (Keel 2013: 981)
4. Scarab 04/K/72/AR1 (Amenhotep III): "probably" K-5 or K-6 (Keel 2013: 979)
5. Scarab 04/K/81b/AR25 (from Ramesses II onward): "probably" K-8 (Keel 2013: 979)
6. Scarab 04/K/105/AR7 (19th–20th Dynasty): "probably" K-8 (Keel 2013: 980)
7. Scarab 04/K/127/AR7 (19th–20th Dynasty): "K-8 but locus is not completely clean" (Keel 2013: 980)
8. Scarab 10/K/35/AR1 (18th Dynasty): "Mixed debris, possibly Level K-10" (Ben-Dor Evian and Münger in press)
9. Scarab 10/K/1/AR10 (22nd Dynasty): found during cleaning in Area K (Ben-Dor Evian and Münger in press)
10. Scarab 10/K/1/AR5 (Thutmose III): found during cleaning (Ben-Dor Evian and Münger in press)
11. Scarab 12/K/12/AR1 (Thutmose IV): "Removal of silo (possibly built in Level K-9)" (Ben-Dor Evian and Münger in press)

In all of the above cases, no secure latest possible layer was provided by the excavators, which prevents us from applying Rule 3 (see "Modeling Rules" above).

[17] Scarabs discarded due to unsecure Egyptian dating are the following:

1. Scarab x 643 (Stratum VI): "most likely" 21st Dynasty (Harrison 2004: 100)
2. Scarab x 792 (Stratum VI): "most likely" 21st Dynasty (Harrison 2004: 100)
3. Scarab x 673 (Stratum VI): seal bearing a motif "rarely" appearing before 19th Dynasty (Harrison 2004: 102)

In all of the above cases, no secure earliest possible reign was provided by the excavators, which prevents us from applying Rule 2 (see "Modeling Rules" above).

[18] Note that the new period does not represent the whole timespan of Philistine Bichrome pottery, but only its presence at Megiddo, which is assumed to have started later (although expectedly not much later) than its appearance in Philistia (e.g., Martin 2017b). This assumption does not reflect on our modeling, however, since our conclusions are limited to Philistine pottery from Megiddo.

Table 2. Egyptian Synchronisms Used in Our Models

Find	*Layer*	*Date*	*Synchronism*	*Reference*
		University of Chicago Excavation		
Ramesses III pen-case	VIIB or VIIA	Ramesses III	VIIA ends after start of Ramesses III	Loud 1939: 9–12
Ramesses VI statue base	VIIA	Ramesses VI	VIIA ends after start of Ramesses VI	Breasted 1948
Scarab	VIIA	Ramesses III	VIIA ends after start of Ramesses III	Loud 1948: 154, pls. 152:195, 158:195; Brandl 2004: 62
Scarab	VIB	Ramesses II	VIB ends after start of Ramesses II	Harrison 2004: 99, no a 495
Scarab	VIA or VIB	Ramesses I	VIA ends after start of Ramesses I	Harrison 2004: 101, no a 529
Scarab	VIA or VIB	Amenhotep III	VIA ends after start of Amenhotep III	Harrison 2004: 101, no d 3
Scarab	IVA or IVB	Ramesses IV	IVA ends after start of Ramesses IV	Lamon and Shipton 1939: pI. 69:27; Brandl 2004: 62
		Area K		
Scarab	K-9	Amenhotep III	K-9 ends after the start of Amenhotep III	Ben-Dor Evian and Münger in press, Scarab 08/K/75/AR1
Scarab	K-8	19th–20th Dynasty	K-8 ends after start of Ramesses I	Keel 2013: 980, Scarab 06/K/91/AR2
Scarab	K-8	Amenhotep II	K-8 ends after start of Amenhotep II	Keel 2013: 978, Scarab 06/K/109/AR2
Scarab	K-7 or K-6	19th–20th Dynasty	K-6 ends after start of Ramesses I	Keel 2013: 980, Scarab 04/K/83a/AR4
		Area H		
Scarab	H-15	18th Dynasty	H-15 ends after start of Ahmose I	Ben-Dor Evian and Münger in press, Scarab 14/H/57/AR1
Scarab	H-9	19th Dynasty	H-9 ends after start of Ramesses I	Keel 2013: 979, Scarab 08/H/6/AR1

consensual duration range of 50 to 200 years has been given to the Bichrome period. In line with the rules defined above, two types of synchronisms are added to the model:

Contemporaneity Synchronisms. The following layers contain Bichrome pottery: Levels K-5–K-4, H-12–H-9, and Strata VIIA–VIA (Finkelstein et al. 2017). They are thus modeled by a simple contemporaneity synchronism between the layer and the new Bichrome period.

Ordered Transitions. In each sequence, the latest layer *before* the appearance of the Bichrome is modeled as: "Layer X ends before the start of Philistine Bichrome." This applies to Levels K-6, H-13, and Stratum VIIB. In the same way, the earliest layer *after* the presence of Bichrome is modeled as "Layer X starts after the end of Philistine Pottery." This applies to Levels K-3, H-8, and Stratum VB.

Figure 8 represents the above data in graphic form.

Radiocarbon Dating

We now wish to integrate into our models the latest radiocarbon results from Areas H and K at Megiddo (see Finkelstein et al. 2017: 274 and **Table 3** below).

Methodological Rules. Radiocarbon results consist of probability distributions, from which date-ranges are extracted by choosing a given confidence level (typically 68.2% or 95.4%). Such date-ranges can be inserted into ChronoLog "as is," since its data model allows direct inclusion of ranges on start and end dates. This approach is even more natural since our stratigraphic sequences (see "Archaeological Periods" above) have been left floating, meaning they do not feature any absolute dates except their 732 B.C.E. termination date. However, caution must be taken before doing so: both OxCal and ChronoLog permit the inclusion of chronological constraints in their models (though in a different way); hence, before inserting OxCal results into our ChronoLog model, we must make sure not to include radiocarbon results depending on Bayesian priors that contradict the inputs of the ChronoLog model. An example of such a contradiction would be an OxCal model featuring a TPQ of 1500 B.C.E. for a given transition, and a ChronoLog model featuring a terminus ante quem (TAQ) of 1600 B.C.E. for the same transition. Furthermore, we must also be aware that ChronoLog is a fully *deterministic* (i.e., non-probabilistic) tool, and hence does not provide probabilities for its computed ranges. In other words, ChronoLog constraints are considered as known hypotheses, and the computed ranges are considered certain under these hypotheses (unless a contradiction is detected). In a way, the

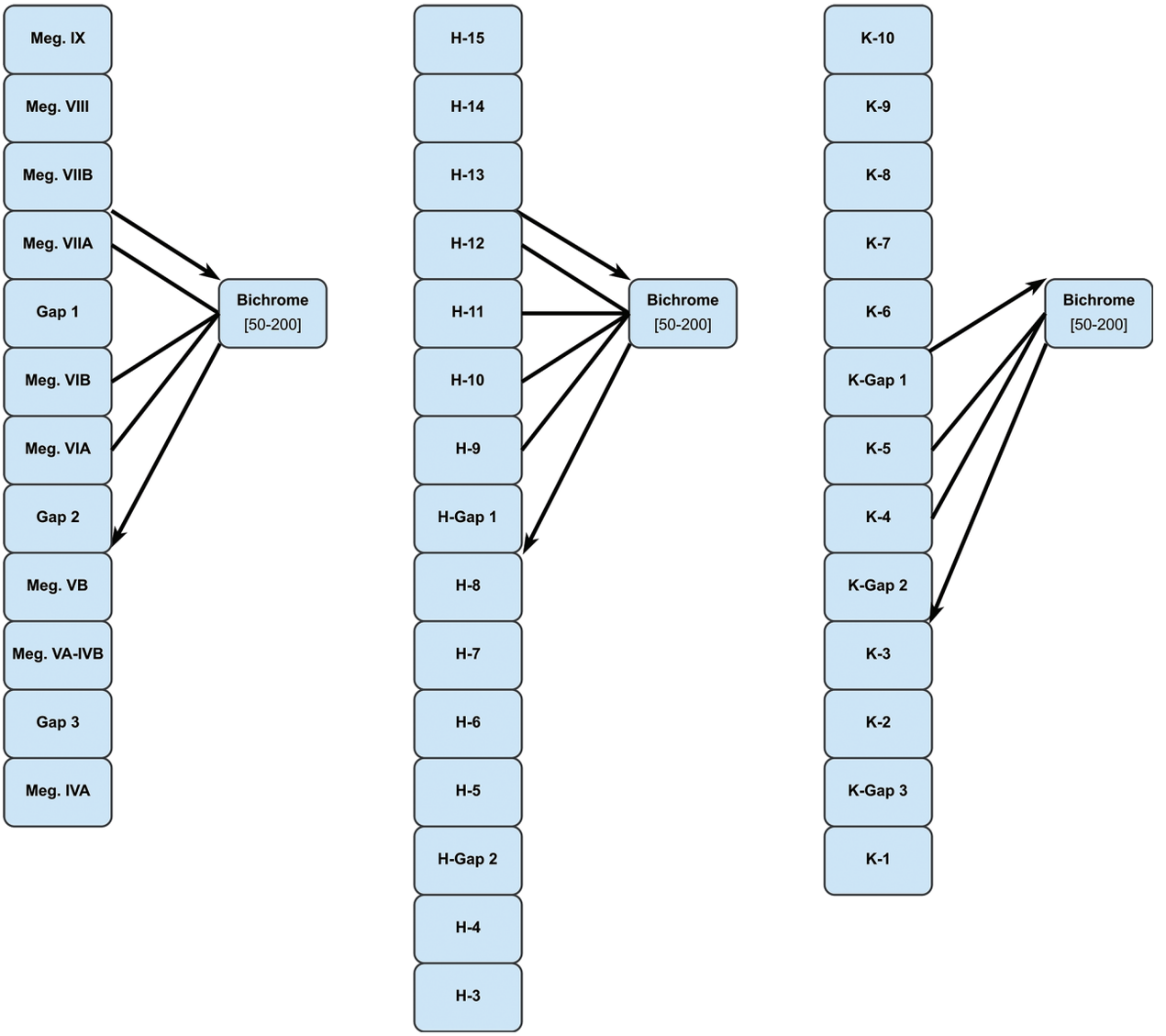

Fig. 8. Philistine pottery in our three stratigraphic sequences. Layers having Bichrome pottery (VIIA to VIA, H-12 to H-9, K-5, to K-4) are modeled with a contemporaneity synchronism, and the layers situated just before and after them (VIIB, VB, H-13, H-8, K-6, and K-3) are modeled with ordered transition synchronisms. (Chart by E. Levy)

inclusion of radiocarbon dates in our ChronoLog models allows us to automate (and formalize) the phase of research usually done after the publication of radiocarbon dates, when these dates are considered a given and researchers discuss their impact on the overall historical/archaeological picture.

Data. The radiocarbon results published in Finkelstein et al. 2017 pertain to the end of Layers K-8–K-5 and H-13–H-10 (see **Table 3**). They are associated with a 68.2% probability, and were obtained by taking the early limit of the end of the phase before each transition and the late limit of the beginning of the phase after that transition.[19] These ranges were obtained using a Bayesian model with only one prior (in addition to relative order of strata), namely the synchronized ending of K-4 and H-9 (Finkelstein et al. 2017: 270), a synchronism that is also included in all our ChronoLog models (see "Archaeological Periods" above). Hence, no contradiction exists between the ChronoLog

[19] See Finkelstein and Piasetzky 2010: 377–78 for a detailed explanation of the dating procedure.

TABLE 3. Radiocarbon Results at 68.2% Confidence Level (from Finkelstein et al. 2017: 274)

Transition	*Range (68.2%)*
Area K	
End K-8/Start K-7	1211–1161
End K-7/Start K-6	1185–1136
End K-6/Start K-5	1136–1083
End K-5/Start K-4	1103–1031
Area H	
End H-13/Start H-12	1146–1084
End H-12/Start H-11	1108–1062
End H-11/Start H-10	1073–1031
End H-10/Start H-9	1047–1011

models and the OxCal model used to obtain the radiocarbon results.[20]

Results

Five experiments were performed on the basis of the above-described data, with the help of ChronoLog. These experiments were conducted using two different models: 1) The "Historical Model," which includes all the data described above in "Megiddo: Data and Modeling Rules," with the exception of radiocarbon results; and 2) The "Radiocarbon Model," comprising all the same data above, including the new Megiddo radiocarbon dates from Areas H and K. These models differ in that the absolute dates calculated in the Historical Model can ultimately derive only from the historical dates of Egyptian pharaohs and from the 732 B.C.E. date for the Assyrian takeover of Megiddo, while the Radiocarbon Model adds many more potential absolute chronology anchors for the calculation of the final dates. The Historical Model will be used for calculating a general TPQ for the appearance of the Bichrome at Megiddo (Result 1), as well as a second TPQ (Result 2) under the additional hypothesis that Stratum VIIB ends after Ramesses III's accession. The Radiocarbon Model will be used to derive both a TPQ (Result 3) and a TAQ (Result 4) for the appearance of the Bichrome at Megiddo. Finally, we will explore the compatibility between the Radiocarbon Model and the hypothesis that Stratum VIIB ends after Ramesses III's accession. The separation of our experiments into two distinct models (Historical and Radiocarbon) will enable us to better assess the precise contribution of radiocarbon dating to the chronological debate regarding Bichrome pottery. Our experiments are described in detail in the following sections, and their results are summarized in **Table 4**.

Result 1: The Bichrome Starts No Earlier than 1183 B.C.E. (Historical Model)

Experiment. The goal of this experiment is to provide the best TPQ for the appearance of Philistine Bichrome pottery at Megiddo based only on historical dates and layer durations.

Results. The result of the experiment is shown in **Figure 9**. The best TPQ computed by ChronoLog for the start of the Bichrome is 1183 B.C.E. It depends on only four inputs: the start date of Ramesses VI, and the bounds on the durations of Stratum VIIA, Level K-7, and Level K-6. The relevant synchronisms are the Ramesses VI statue from Stratum VIIA, the synchronized ending of VIIB and K-8, and Stratum K-6 ending before the start of the Bichrome. The final figure of 1183 B.C.E. is obtained thus:

$$\begin{aligned} &start(Ramesses\ VI) - max.\,duration(VIIA) \\ &\quad + min.\,duration(K\text{-}7) + min.\,duration(K\text{-}6) \\ &\quad = -1143 - 100 + 10 + 50 \\ &\quad = -1183. \end{aligned}$$

This provides a useful algebraic expression, as it enables us to recompute the TPQ if other estimates are given for the durations of Stratum VIIA and Levels K-7 or K-6. For example, setting an 80 years combined minimum duration for Levels K-7 and K-6 (instead of 60) would yield a TPQ of 1163 instead of 1183 B.C.E. It is also interesting to note that among the hundreds of encoded data, only four periods and three synchronisms were necessary for obtaining the optimal TPQ for the start of the Bichrome, thus showing the strength of ChronoLog for pointing to the relevant data among complex chronological networks. Note that this does not imply that the other data have no impact at all, since they do influence other periods. For example, they help narrow down the durations and absolute dates of each layer.

Result 2: The Bichrome Starts No Earlier than 1124 B.C.E. (Historical Model with Stratum VIIB Ending after Ramesses III's Accession)

Experiment. Our second experiment is also done on the basis of the Historical Model (hence without radiocarbon), but with an updated synchronism regarding the Ramesses III pen-case from Stratum VII. We saw in "Egyptian Synchronisms" above that the exact placement of the

[20] We have also tried rerunning OxCal without this one prior (synchronized ending of K-4 and H-9) and obtained results almost identical to those obtained with the prior, hence our usage of the published dates "as is."

Table 4. Summary of Results Using Kitchen's (2000) Egyptian Chronology

	Model	*Question*	*Result*
1	Historical	Best TPQ for the start of the Bichrome	Bichrome starts no earlier than 1183 B.C.E.
2	Historical	Best TPQ for the start of the Bichrome, assuming Stratum VIIB ends after Ramesses III's accession	Bichrome starts no earlier than 1124 B.C.E.
3	Radiocarbon	Best TPQ for the start of the Bichrome	Bichrome starts no earlier than 1111 B.C.E.
4	Radiocarbon	Best TAQ for the start of the Bichrome	Bichrome starts no later than 1086 B.C.E.
5	Radiocarbon	Does Stratum VIIB end before or after Ramesses III's accession?	Stratum VIIB ends after Ramesses III's accession

pen-case within Stratum VII (VIIB or VIIA) is unknown. We had thus modeled it as "Meg. VIIA ends after the start of Ramesses III," since our Rule 3 (see above) stated that the *latest* layer must be taken in cases of stratigraphic uncertainty. We now wish to explore the chronological implications of a Stratum VIIB origin for the pen-case, hence the inclusion of the following new synchronism in our model: "Meg. VIIB ends after the start of Ramesses III."

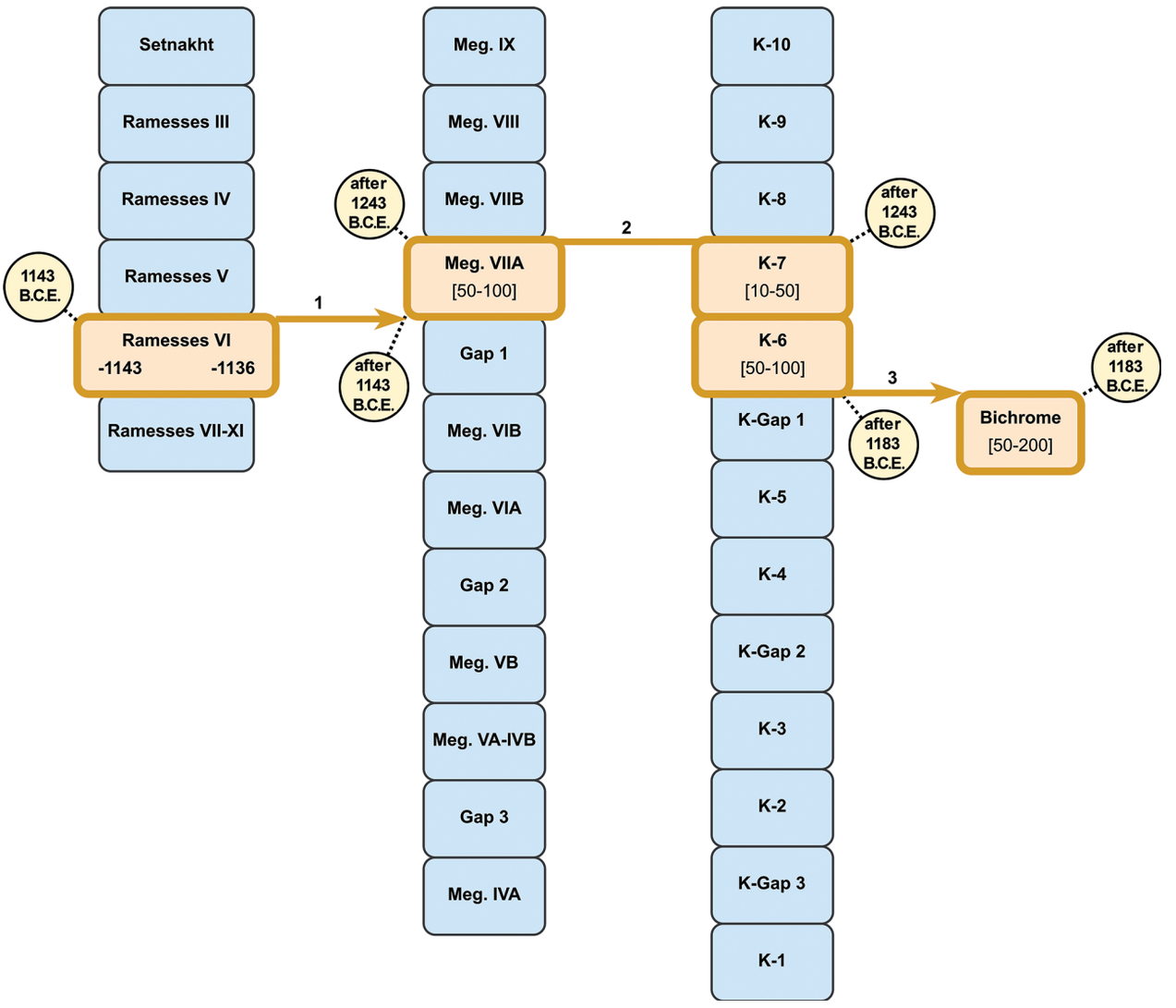

Fig. 9. Result 1: Bichrome starts no earlier than 1183 B.C.E. under the Historical Model. (Chart by E. Levy)

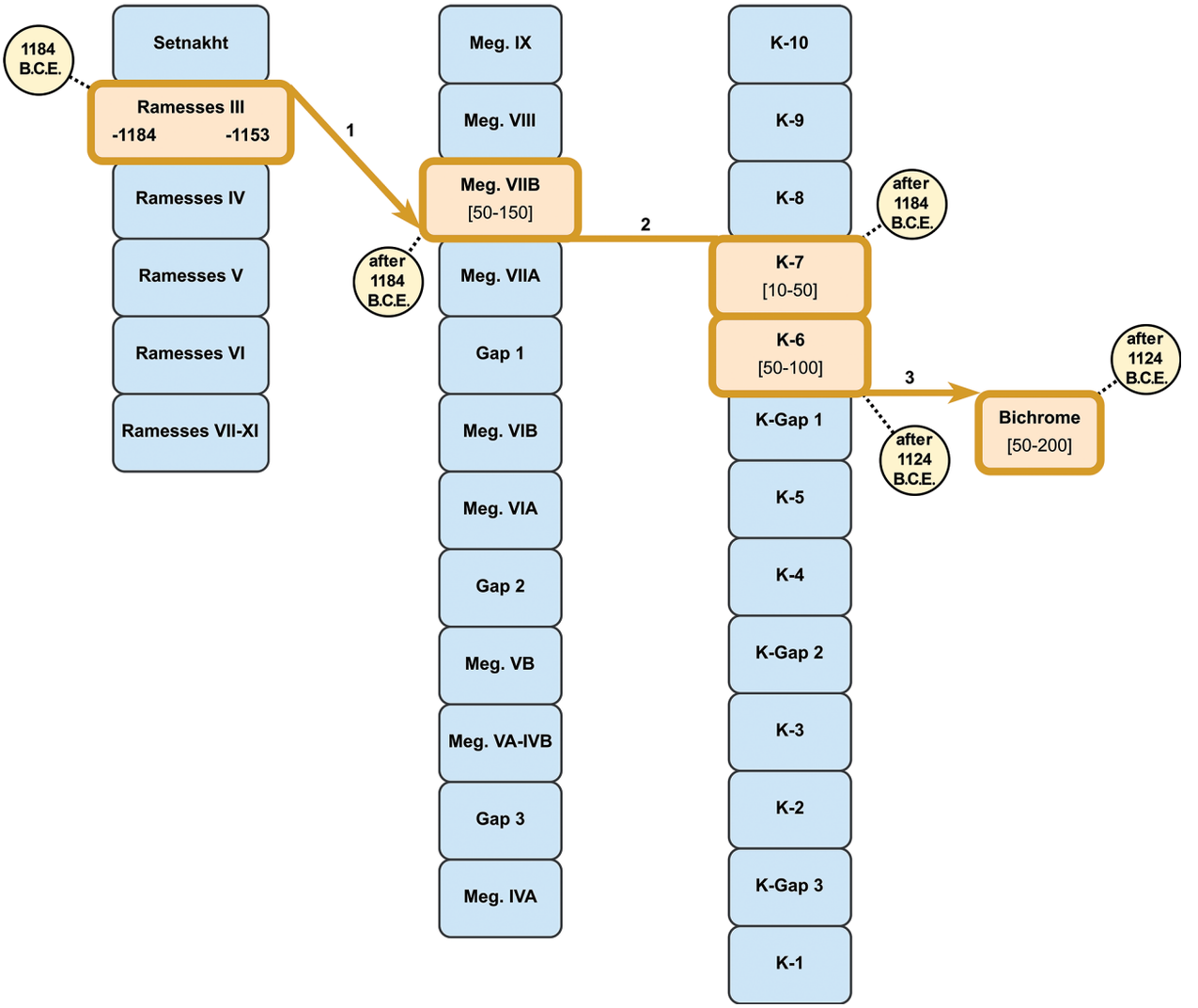

Fig. 10. Result 2: Bichrome starts no earlier than 1124 B.C.E. under the Historical Model, assuming Stratum VIIB ends after Ramesses III's accession. (Chart by E. Levy)

Results. The result of the experiment is shown in **Figure 10**. The best TPQ for the start of the Bichrome is now 1124 B.C.E. It depends on four inputs: the start date of Ramesses III, and the bounds on the durations of Stratum VIIB, Level K-7, and Level K-6. The relevant synchronisms are the Ramesses III pen-case set in Stratum VIIB, the synchronized ending of VIIB and K-8, and Level K-6 ending before the start of the Bichrome. The final figure of 1124 B.C.E. is obtained thus:

$$\begin{aligned} &start(Ramesses\ III) + min.\ duration(K\text{-}7) \\ &\quad + min.\ duration(K\text{-}6) = -1184 + 10 + 50 \\ &\quad = -1124. \end{aligned}$$

Here again, as in the previous model, the above algebraic expression allows us to adapt the final result if minimum durations other than 10 and 50 are set for Levels K-7 and K-6. Note that the result of 1124 B.C.E. depends on very few pieces of data (four periods and three synchronisms) and provides a low date, in fact lower than the 1136 cal B.C.E. TPQ for the end of K-6 obtained in Finkelstein et al. 2017 through radiocarbon alone. This result strongly puts into perspective the contribution of radiocarbon to our debate. This aspect, as well as the archaeological relevance of Stratum VIIB being still in use after the start of Ramesses III's reign are discussed in "Result 5" below.[21]

[21] Note that the above result only relies on the question of whether Stratum VIIB was still standing when Ramesses III came to power, meaning the result holds if Stratum VIIB ends after the start of Ramesses III, even if the pen-case itself actually belonged to Stratum VIIA.

Result 3: The Bichrome Starts No Earlier than 1111 B.C.E. (Radiocarbon Model)

Experiment. Our third experiment is done on the basis of the Radiocarbon Model. This model is based on the Historical Model augmented with radiocarbon dates from Areas K and H (see "Radiocarbon Dating" above). These radiocarbon results (68% probability) were inserted as ranges on start and end dates of Levels K-8 to K-4 and H-13 to H-9. Our goal is to provide the best TPQ for the appearance of Philistine pottery at Megiddo, based on a combination of these radiocarbon results with our set of synchronisms and layer durations.

Results. The result of the experiment is shown in **Figure 11**. The best TPQ for the start of the Bichrome in this model is 1111 B.C.E., hence providing a tighter (i.e., later) result than the previous 1124 B.C.E. result (Result 2). It depends on five inputs: the radiocarbon TPQ for the start of Level H-12 (1146 cal B.C.E.), and the bounds on the durations of Levels H-11, K-7, K-6, and Stratum VIIA. The relevant synchronisms are the synchronized endings of Levels H-11 and K-8 with Strata VIIB and VIIA respectively, as well as Stratum K-6 ending before the start of the Bichrome. Note that only one radiocarbon result (start of Level H-12) was necessary to obtain our TPQ. The result is more complex than in the two previous models since in

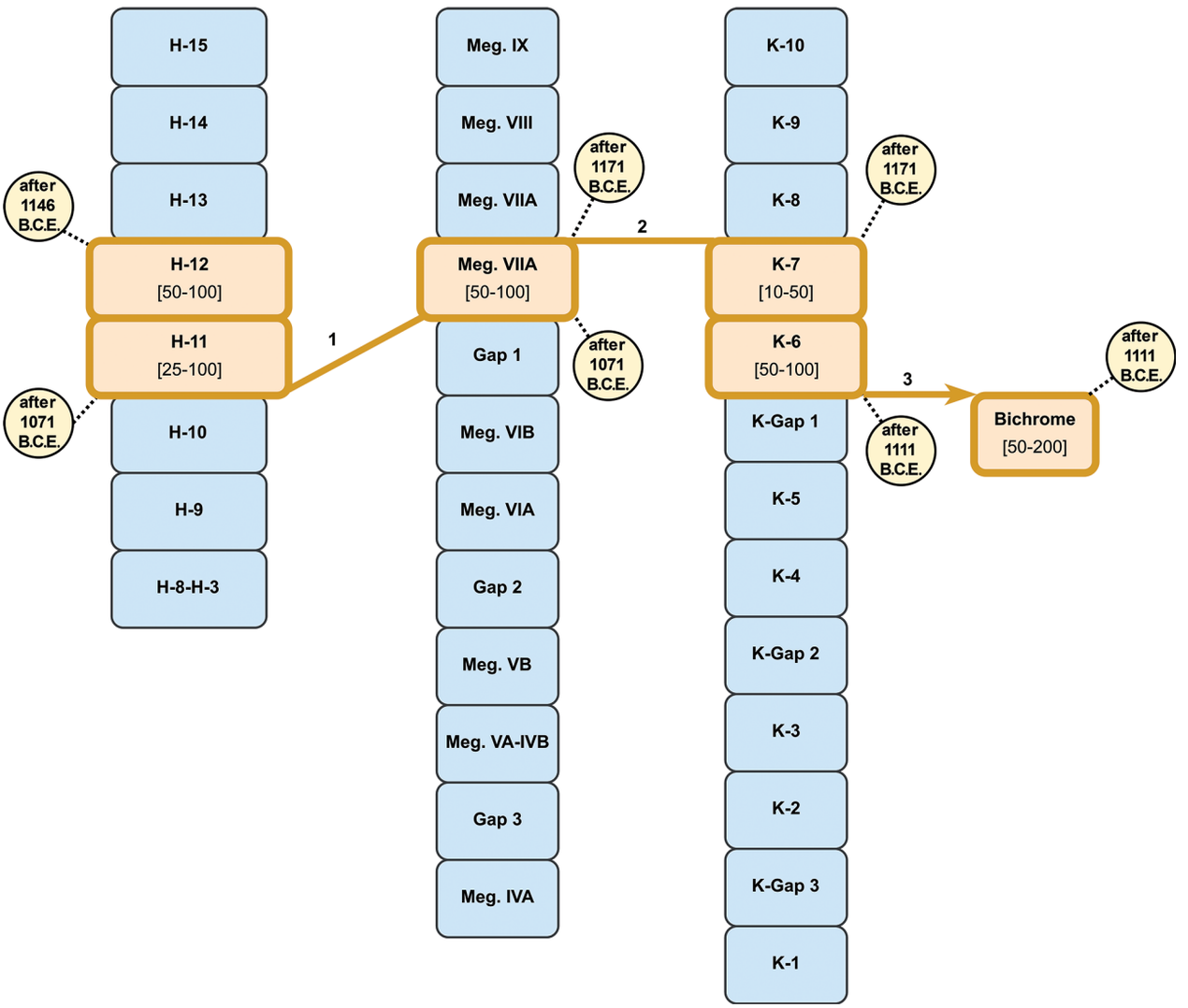

Fig. 11. Result 3: Bichrome starts no earlier than 1111 B.C.E. under the Radiocarbon Model. (Chart by E. Levy)

this case the final date depends on all three stratigraphic sequences (University of Chicago and Areas K and H). It is thus even more complex to spot manually. The final figure of 1111 B.C.E. is obtained thus:

$$\begin{aligned} &earliest\ start(H\text{-}12) + min.\ duration(H\text{-}12) \\ &\quad + min.\ duration(H\text{-}11) - max.\ duration(VIIA) \\ &\quad + min.\ duration(K\text{-}7) + min.\ duration(K\text{-}6) \\ &\quad = -1146 + 50 + 25 - 100 + 10 + 50 = -1111. \end{aligned}$$

This result is later than the 1136 cal B.C.E. result obtained by radiocarbon alone (Finkelstein et al. 2017), stemming from the fact that our model adds several input data absent from the original OxCal model, such as layer durations and additional synchronisms.

Result 4: The Bichrome Starts No Later than 1086 B.C.E. (Radiocarbon Model)

Experiment. In this fourth experiment, the model is exactly the same as in the previous experiment (Radiocarbon Model), but we are searching for a TAQ for the appearance of Bichrome pottery at Megiddo, rather than a TPQ.

Results. The result of the experiment is shown in **Figure 12**. The best TAQ for the start of the Bichrome in the Radiocarbon Model is 1086 B.C.E. It depends on three

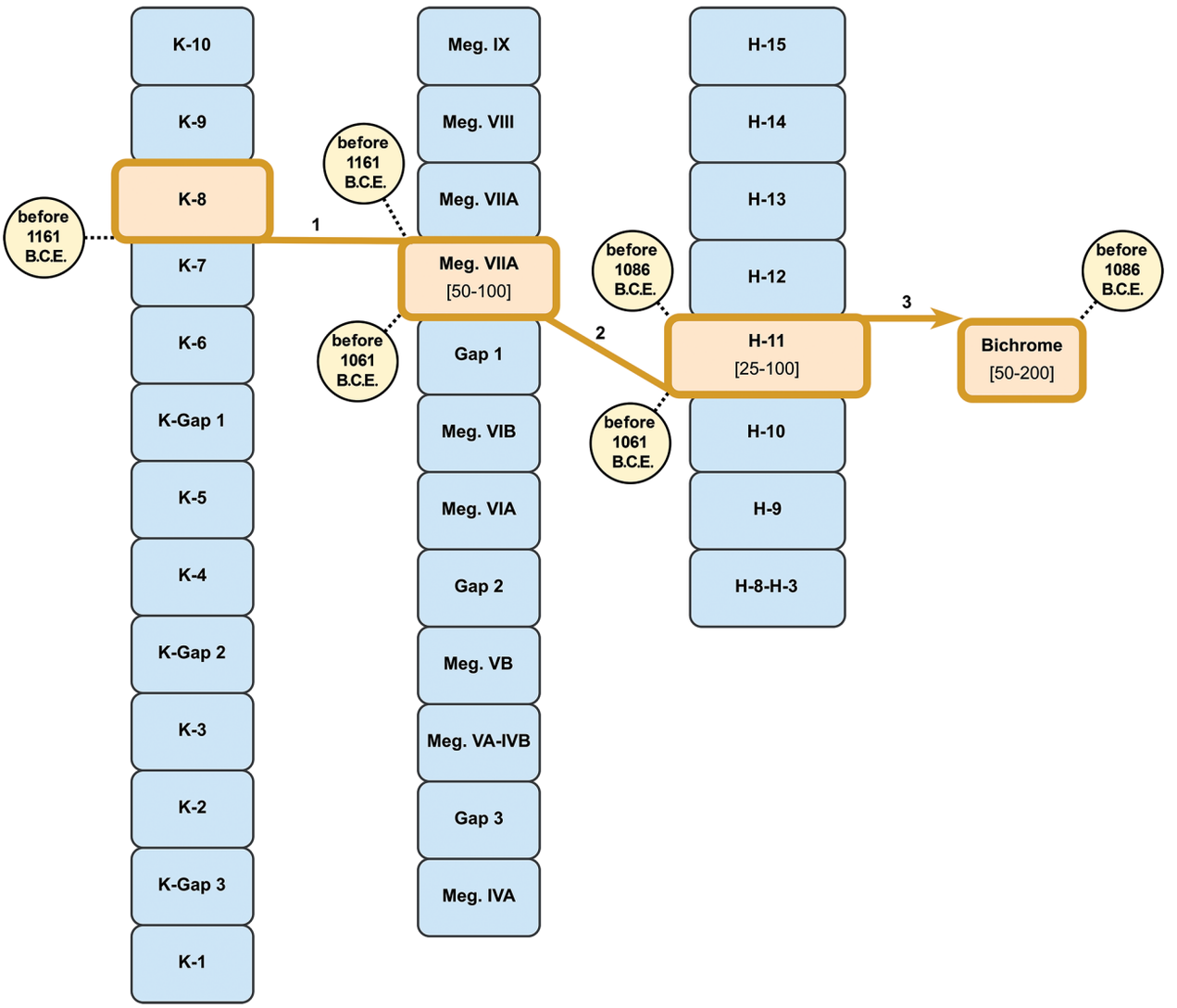

Fig. 12. Result 4: Bichrome starts not later than 1086 B.C.E. under the Radiocarbon Model. (Chart by E. Levy)

inputs: the radiocarbon TAQ for the end of Level K-8 (1161 cal B.C.E.), and the bounds on the durations of Level H-11 and Stratum VIIA. The relevant synchronisms are the synchronized endings of Levels H-11 and K-8 with Strata VIIA and VIIB respectively, as well as Level H-11 starting before the start of the Bichrome.[22] This TAQ result, coupled with the preceding TPQ of 1111 B.C.E., gives us a narrow window for the appearance of Bichrome pottery at Megiddo, namely 1111–1086 B.C.E.—a 25-year range. This very precise result was attained by a combination of all the input data of our ChronoLog model with the radiocarbon results for Areas H and K. Note that only one radiocarbon result was necessary here (end of Level K-8) to obtain our TAQ. Here again, the result can also be expressed algebraically. The final figure of 1086 B.C.E. is obtained thus:

$$\begin{aligned} &latest\ end(K\text{-}8) + max.\ duration(VIIA) \\ &\quad - min.\ duration(H\text{-}11) = -1161 + 100 - 25 \\ &\quad = -1086. \end{aligned}$$

Result 5: Stratum VIIB Ends after Ramesses III's Accession (Radiocarbon Model)

Experiment. The goal of this experiment is to test, within the Radiocarbon Model, whether Stratum VIIB ended after Ramesses III's accession or before it. This question is debated since the only data provided by the University of Chicago excavations is that the Ramesses III pen-case originated from Stratum VII (undivided). We therefore wish to use ChronoLog once again as a hypothesis testing device, in order to check whether the reign of Ramesses III could have started as early as Stratum VIIB. In other words, we wish to test whether the main hypothesis of our second experiment (see "Result 2" above) is compatible with the radiocarbon results of Areas K and H. This is an important question since the addition of this hypothesis yielded a much later TPQ than in the simple Historical Model (1124 B.C.E. as opposed to 1183 B.C.E.). We thus test this hypothesis here by adding the following new synchronism to the Radiocarbon Model: "Stratum VIIB ends *before* the start of Ramesses III," and checking whether ChronoLog detects a contradiction.

Results. The result of the experiment is that the inclusion of the new synchronism "Stratum VIIB ends before the start of Ramesses III" yields a contradiction, detected by ChronoLog. This contradiction is explained thus (see **Fig. 13**): the radiocarbon TPQ for the start of Level H-12 (1146 cal B.C.E.), coupled with Levels H-12 and H-11 and Stratum VIIA duration estimates and the Level H-11 synchronized ending with Stratum VIIA, imply a 1171 B.C.E. TPQ for the start of Ramesses III, which is in contradiction with his 1184 B.C.E. accession date. Hence, the reign of Ramesses III must start *before* the end of Stratum VIIB (under the Radiocarbon Model). This contradiction result reinforces, with the help of radiocarbon, the hypothesis that Stratum VIIB was still standing at the start of Ramesses III's reign, a hypothesis independently defended recently by Martin (2017a: 283) on purely archaeological grounds. This result is important since, as argued above ("Result 2"), if verified, it implies a low TPQ (1124 B.C.E.) for the start of Bichrome pottery at Megiddo, even without using radiocarbon results.

Experiments with Thomas Schneider's High Egyptian Chronology

All the above-described models relied on Kitchen's Egyptian chronology (2000, see **Table 2**). We have also run our experiments using a higher Egyptian chronology (Schneider 2010, see **Table 5**). Only two of our five results were affected by this change (see **Table 6**): Result 1 became 1192 B.C.E. instead of 1183 B.C.E. (due to Schneider's 1152 B.C.E. accession date for Ramesses VI, instead of Kitchen's 1143 B.C.E.) and Result 2 became 1135 B.C.E. instead of 1124 B.C.E. (due to Schneider's 1195 B.C.E. accession date for Ramesses III, instead of Kitchen's 1184 B.C.E.). The other results remained unchanged. Results 3 and 4 indeed rely only on radiocarbon dates and not on historical dates, and hence were not affected. Finally, Result 5 remains valid as well. Indeed, this result rested on a contradiction between the 1184 B.C.E. accession date of Ramesses III and the 1171 B.C.E. TPQ computed by ChronoLog. This contradiction becomes even stronger using Schneider's 1195 B.C.E. accession date for Ramesses III.

Experiments with 95.4% Radiocarbon Confidence Level

The above results were obtained using the 68.2% confidence intervals as reported in Finkelstein et al. 2017. Their article did not report any 95.4% confidence intervals. As a sensitivity check, we reran OxCal to obtain them (**Table 7**) and then inserted them into our ChronoLog model. The results are shown in **Table 8**. Regarding the start of the Bichrome (Results 3 and 4), the new range (1128–1079 B.C.E.) is close to the old one (1111–1086 B.C.E.) and thus still supports a late appearance of the Bichrome at Megiddo. Regarding the overlap of Stratum VIIB and Ramesses III (Result 5), the stratum's earliest end is now 1188 B.C.E. instead of 1171 B.C.E. This indicates that VIIB

[22] This synchronism follows from the fact that Level H-12 is contemporaneous with the Bichrome, hence H-12 ends after the start of the Bichrome, hence H-11 starts after the start of the Bichrome (as the end of H-12 equals the start of H-11).

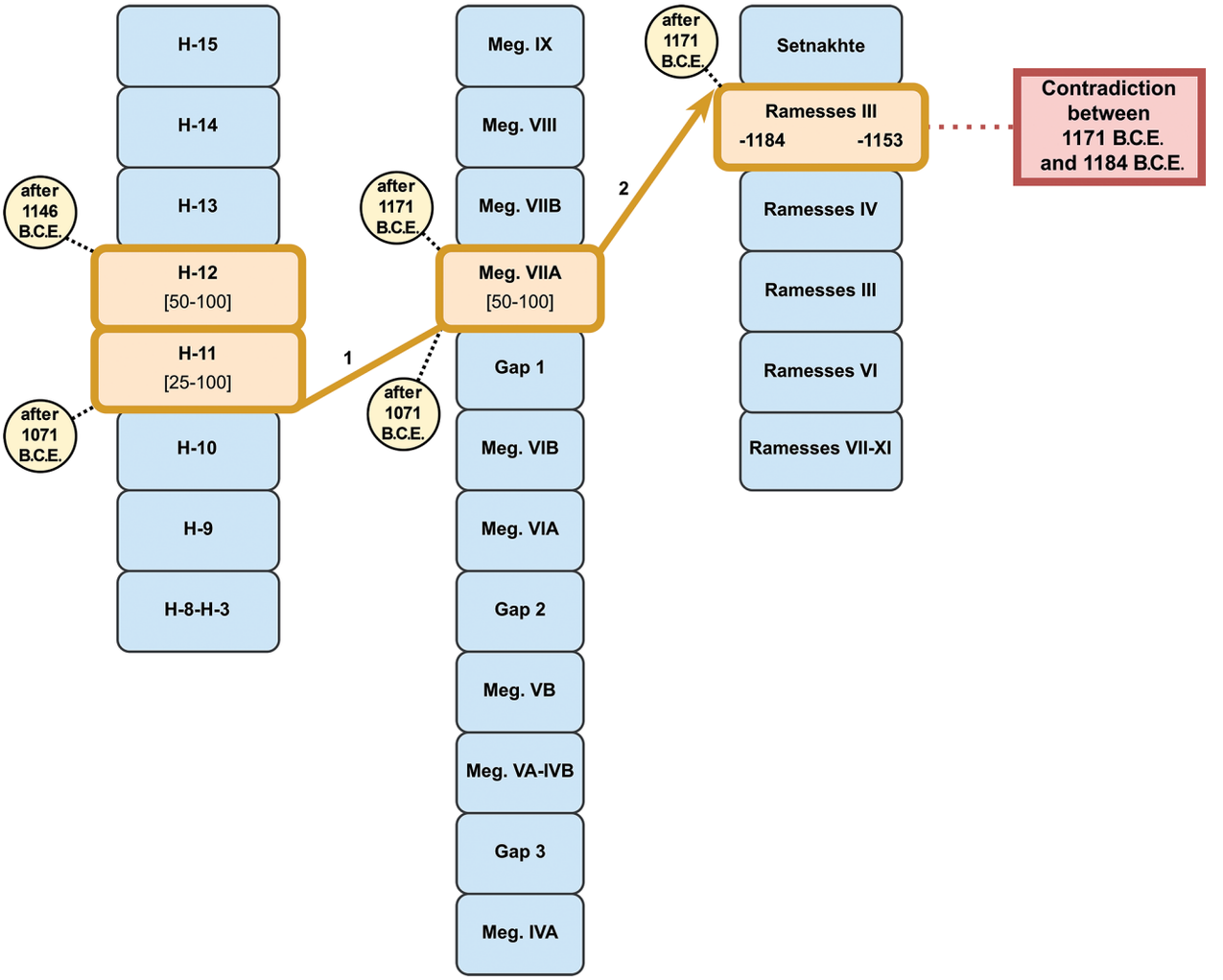

Fig. 13. Result 5: the reign of Ramesses III starts before the end of Stratum VIIB, under the Radiocarbon Model. (Chart by E. Levy)

ends either after Ramesses's accession (1184 B.C.E.) or only slightly before (by at most 4 years).

Discussion

The results presented above consisted of three TPQs and one TAQ for the start of the Philistine Bichrome at Megiddo, and one incompatibility result. They can be summarized as follows:

Without radiocarbon, we have a TPQ of 1183 B.C.E. for the start of Bichrome pottery at Megiddo. This TPQ is lowered to 1124 B.C.E. if we hypothesize that Ramesses III came to power before the end of Stratum VIIB.

With radiocarbon (at 68.2% confidence level), we have a range of 1111–1086 B.C.E. for the start of the Bichrome at Megiddo. Note that this is a very tight range, of only 25 years, and that it is situated at the 12th–11th century transition, thus confirming the conclusions expressed in Finkelstein et al. 2017. With a 95.4% confidence level, the range widens to 1128–1079 B.C.E., which still represents a low date for the start of the Bichrome.

An ending of Stratum VIIB before Ramesses III's accession (1184 B.C.E.) is incompatible with the new 68.2% radiocarbon ranges. Taking the 95.4% ranges, Stratum VIIB could have ended before Ramesses III, but not more than four years before. These results suggest a lower date for the end of Stratum VIII than usually assumed (see, for example, Kempinski's estimate of 1250 B.C.E. [1989: 10, 76–77], later lowered by Finkelstein to 1200 B.C.E. [1996: 171–72]).

These results are in favor of an appearance of Bichrome at Megiddo around the 12th–11th century transition (see also Finkelstein et al. 2017: 276). The termination of Stratum VIIB after (or only slightly before) Ramesses III's accession is an additional result which, interestingly, was recently independently claimed, on purely archaeological grounds (i.e., without radiocarbon or computational models) by Martin (2017a).

Table 5. Absolute Chronology of the 18th, 19th, and 20th Egyptian Dynasties (Schneider 2010)

18th Dynasty	
Ahmose I	1548–1523
Amenhotep I	1523–1502
Thutmose I	1502–1489
Thutmose II	1489–1476
Hatshepsut/Thutmose III	1476–1422
Amenhotep II	1422–1396
Thutmose IV	1396–1386
Amenhotep III	1386–1348
Amenhotep IV	1348–1331
Transition period	1331–1327
Tutankhamun	1327–1318
Ay	1318–1315
Horemheb	1315–1301
19th Dynasty	
Ramesses I	1301–1300
Seti I	1300–1290
Ramesses II	1290–1224
Merneptah	1224–1214
Seti II	1214–1208
Amenmesse	1208–1206
Siptah and Twosret	1206–1198
20th Dynasty	
Sethnakhte	1198–1195
Ramesses III	1195–1164
Ramesses IV	1164–1156
Ramesses V	1156–1152
Ramesses VI	1152–1144
Ramesses VII–XI	1144–1086

The main difference between former chronology work and ours is that here, the proposed results have been obtained in a *fully deductive* and computational manner, and with a *full disclosure* of all the base hypotheses involved. Furthermore, we provide, perhaps for the first time, a clear evaluation of the intrinsic contribution of radiocarbon to the debate by separately presenting the historically based chronological results and those obtained via radiocarbon. This separation allows us to discover that, under the hypothesis of accession of Ramesses III during Stratum VIIB, we can obtain a late TPQ for the Bichrome, namely 1124 B.C.E., thus lowering the 1136 B.C.E. TPQ obtained via OxCal alone (Finkelstein et al. 2017: 274), even without resorting to radiocarbon.[23] We believe that these results strongly argue for the systematic use of such a separated historical/radiocarbon approach in papers presenting radiometric results pertaining to historical periods.

Another advantage of our method is that, in case of disagreement with one of our ground hypotheses (say, a duration estimate), one can easily change that hypothesis in ChronoLog and check the impact of the change on the global model. This puts general (i.e., not only radiocarbon-based) chronological debates on a rigorous computational footing, since the impact of any divergent set of views between scholars can now be evaluated immediately in a formal and objective way. To the best of our knowledge, this is the first such general tool for a deterministic (i.e., non-statistical) evaluation of ancient chronologies. ChronoLog thus provides a useful complementary tool to OxCal, by allowing a fuller (and deterministic) integration of any dating estimate (radiometric or other), duration estimate, and synchronism into the greater historical/archaeological network.

The results presented above are only those pertaining to the Bichrome phase at Megiddo. Nevertheless, ChronoLog produced many other interesting results. Among these, within the Historical Model (see **Appendix B**), one can see some very short duration ranges, such as 85–100 years for Stratum VIIA, 10–25 years for Level K-7, 50–65 years for Level K-6, and 25–40 years for Level H-11. These duration results are also valid under the hypothesis that Stratum VIIB ends after Ramesses III's accession (see **Appendix C**). Even more precise results are obtained within the Radiocarbon Model, among which are 10-year precision ranges[24] for the end of specific periods, such as: 1171–1161 B.C.E. for Stratum VIIB and Level K-8, 1071–1061 B.C.E. for Stratum VIIA, 1146–1136 B.C.E. for Level H-13, 1096–1086 B.C.E. for Level H-12, 1071–1061 B.C.E. for Level H-11, and 1146–1136 B.C.E. for the LB IIB (using the 68.2% radiocarbon ranges, see **Appendix D**). The fact that these ranges are tighter than the ones obtained via OxCal alone (see **Table 3**) is due to the fact that the ChronoLog model included many more constraints than OxCal. Indeed, the very fast computation time of ChronoLog (see "Functionalities of the Software") encourages the building and testing of larger models than with OxCal alone, as the latter requires long execution times due to complex probabilistic computation. Our models, featuring 78 periods, over 100 synchronisms, and over 100 duration/date constraints, ran within one second on a standard personal computer. When dealing with radiocarbon results, we therefore propose a two-step methodology: the use of OxCal models to obtain reliable ranges

[23] This observation also holds if we use Schneider's high Egyptian chronology (see above). In this case, the Historical Model with the hypothesis of Stratum VIIB ending after Ramesses III's accession yields a TPQ of 1135 B.C.E. (instead of 1124 B.C.E.), which is still as good as the 1136 B.C.E. TPQ obtained via radiocarbon alone.

[24] All these 10-year ranges ultimately depend on only two radiocarbon dates: the 1146 B.C.E. TPQ for the end of Level H-13 and the 1161 TAQ for the end of Level K-8 (see **Table 3**), coupled with the relevant synchronisms and duration estimates.

Table 6. Summary of Results Using Schneider's (2010) Egyptian Chronology

	Model	*Question*	*Result**
1	Historical	Best TPQ for the start of the Bichrome	Bichrome starts no earlier than 1192 B.C.E.
2	Historical	Best TPQ for the start of the Bichrome, assuming Stratum VIIB ends after Ramesses III's accession	Bichrome starts no earlier than 1135 B.C.E.
3	Radiocarbon	Best TPQ for the start of the Bichrome	Bichrome starts no earlier than 1111 B.C.E.
4	Radiocarbon	Best TAQ for the start of the Bichrome	Bichrome starts no later than 1086 B.C.E.
5	Radiocarbon	Does Stratum VIIB end before or after Ramesses III's accession?	Stratum VIIB ends after Ramesses III's accession

*Only Results 1 and 2 differ from the results obtained using Kitchen's (2000) chronology

on the desired phases, and the later introduction of these results (considered safe) into ChronoLog in order to evaluate how they fit into the global historical/archaeological picture.

Another interesting aspect of the ChronoLog approach presented here is its ability to *sort* between a multitude of data in order to identify which ones really do impact the problem under investigation. In our case, we were able to detect that in the Historical Model (see "Result 1"), the final TPQ for the start of the Bichrome was only influenced by one historical date (Ramesses VI's accession date) and three duration estimates (for Stratum VIIA and Levels K-7 and K-6). Under the Radiocarbon Model (at 68.2% confidence level), the final TPQ rested on one OxCal radiocarbon result, 1146 B.C.E., for the end of Level H-13 and five duration estimates (for Stratum VIIA and Levels H-12, H-11, K-7, and K-6). These precise sources for the final TPQs are extremely difficult to detect manually, given the large number of periods (78) and synchronisms (over 100) involved. This particular ability of ChronoLog to sort between the relevant and non-relevant data is of great importance, since it can guide the archaeologist as to which layers have the greatest potential chronological impact and hence deserve the greatest attention.

Note also that some of our ground data, such as the sequence of archaeological periods and the 732 B.C.E. end date of our three stratigraphic sequences, bore no impact on any of the five main results presented here. This does not mean that they have no effect whatsoever. For example, the sequence of archaeological periods does have a significant impact on the tightening of some duration ranges of our layers (see **Appendices B–D** for these final ranges). On the other hand, it is also possible that some specific data have no effect at all on a given ChronoLog model. For example, under the Historical Model, taking the 18th Dynasty out of the picture (with all its associated synchronisms) has no effect on any start date, end date, or duration—a result not easy to spot manually.

Our models could be refined further by the inclusion of additional foreign artifacts, most notably Mycenaean and Cypriot ceramic imports, which are abundant at Megiddo. In the same way, the question of the date of appearance of Philistine Bichrome pottery could be extended to a wider region, by inclusion of other relevant sites to our models, such as Jaffa (Burke et al. 2017), Qubur el-Walaydah (Asscher, Lehmann et al. 2015), and Tell es-Safi/Gath (Asscher, Cabanes et al. 2015). These two important questions are left for future works.

Table 7. Radiocarbon Results with 95.4% Confidence Level (Based on Finkelstein et al. 2017: 272, Table 1)

Transition	*Range (95.4%)*
Area K	
End K-8/Start K-7	1217–1143
End K-7/Start K-6	1197–1131
End K-6/Start K-5	1160–1056
End K-5/Start K-4	1115–1018
Area H	
End H-13/Start H-12	1165–1051
End H-12/Start H-11	1115–1045
End H-11/Start H-10	1088–1020
End H-10/Start H-9	1063–1004

Acknowledgments

Eythan Levy was supported by the Center for Absorption in Science, the Ministry of Absorption, the State of Israel, and by the Dan David Foundation. The study was also supported by Mr. Jacques Chahine, through the French Friends of Tel Aviv University.

Table 8. Summary of the Radiocarbon Model Sensitivity Test Using 95.4% Confidence Level

Question	*Result*
Best TPQ for the start of the Bichrome	Bichrome starts no earlier than 1128 B.C.E.
Best TAQ for the start of the Bichrome	Bichrome starts no later than 1079 B.C.E.
Does Stratum VIIB end before or after Ramesses III's accession?	Stratum VIIB ends within the range 1188–1144 B.C.E., thus either after Ramesses III's accession (1184 B.C.E.) or at most 4 years before it

Appendix A: Comprehensive List of Synchronisms (Historical and Radiocarbon Models)

No.	*Period 1*	*Synchronism*	*Period 2*
		Stratigraphic Synchronisms	
1	Megiddo K-4	*ends at the same time as*	Megiddo H-9
2	Megiddo K-8	*ends at the same time as*	Megiddo VIIB
3	Megiddo K-4	*ends at the same time as*	Megiddo VIA
4	Megiddo H-11	*ends at the same time as*	Megiddo VIIA
5	Megiddo H-9	*ends at the same time as*	Megiddo VIA
6	Megiddo H-5	*ends at the same time as*	Megiddo K-2
		Archaeological Periods (LB)	
7	Megiddo H-15	*is contemporaneous with*	LB I
8	Megiddo K-10	*is contemporaneous with*	LB I
9	Megiddo IX	*is contemporaneous with*	LB I
10	Megiddo H-14	*is contemporaneous with*	LB IIA
11	Megiddo K-9	*is contemporaneous with*	LB IIA
12	Megiddo VIII	*is contemporaneous with*	LB IIA
13	Megiddo K-8	*is contemporaneous with*	LB IIB
14	Megiddo K-7	*is contemporaneous with*	LB IIB
15	Megiddo VIIB	*is contemporaneous with*	LB IIB
16	Megiddo H-13	*is contemporaneous with*	LB IIB
17	Megiddo K-6	*is contemporaneous with*	LB III
18	Megiddo H-12	*is contemporaneous with*	LB III
19	Megiddo VIIA	*is contemporaneous with*	LB III
20	Megiddo IX	*ends before the start of*	LB IIB
21	Megiddo VIII	*starts after the end of*	LB I
22	Megiddo VIII	*ends before the start of*	LB III
23	Megiddo VIIB	*starts after the end of*	LB IIA
24	Megiddo VIIA	*starts after the end of*	LB IIA
25	Megiddo VIB	*starts after the end of*	LB III
26	Megiddo H-15	*starts after the start of*	LB I
27	Megiddo H-13	*starts after the end of*	LB IIA
28	Megiddo H-13	*ends before the start of*	LB III
29	Megiddo H-12	*starts after the end of*	LB IIB
30	Megiddo H-11	*starts after the end of*	LB III
31	Megiddo H-10	*starts after the end of*	LB III
32	Megiddo H-9	*starts after the end of*	LB III
33	Megiddo H-8	*starts after the end of*	LB III
34	Megiddo K-9	*starts after the end of*	LB I
35	Megiddo K-9	*ends before the start of*	LB IIB
36	Megiddo K-8	*starts after the end of*	LB IIA
37	Megiddo K-8	*ends before the start of*	LB III
38	Megiddo K-7	*starts after the end of*	LB IIA
39	Megiddo K-7	*ends before the start of*	LB III
40	Megiddo K-5	*starts after the end of*	LB III
41	Megiddo K-4	*starts after the end of*	LB III
		Archaeological Periods (Iron Age)	
42	Megiddo K-5	*is contemporaneous with*	Early Iron I
43	Megiddo H-12	*is contemporaneous with*	Early Iron I
44	Megiddo H-11	*is contemporaneous with*	Early Iron I
45	Megiddo H-10	*is contemporaneous with*	Early Iron I
46	Megiddo VIB	*is contemporaneous with*	Early Iron I
47	Megiddo K-4	*is contemporaneous with*	Late Iron I
48	Megiddo H-9	*is contemporaneous with*	Late Iron I

No.	*Period 1*	*Synchronism*	*Period 2*
49	Megiddo VIA	*is contemporaneous with*	Late Iron I
50	Megiddo H-8	*is contemporaneous with*	Early Iron IIA
51	Megiddo VB	*is contemporaneous with*	Early Iron IIA
52	Megiddo H-5	*is contemporaneous with*	Late Iron IIA
53	Megiddo K-2	*is contemporaneous with*	Late Iron IIA
54	Megiddo VA-IVB	*is contemporaneous with*	Late Iron IIA
55	Megiddo H-4	*is contemporaneous with*	Iron IIB
56	Megiddo H-3	*is contemporaneous with*	Iron IIB
57	Megiddo K-1	*is contemporaneous with*	Iron IIB
58	Megiddo IVA	*is contemporaneous with*	Iron IIB
59	Megiddo VIIB	*ends before the start of*	Early Iron I
60	Megiddo VIA	*ends before the start of*	Early Iron IIA
61	Megiddo VB	*starts after the end of*	Late Iron I
62	Megiddo VB	*ends before the start of*	Iron IIB
63	Megiddo VA-IVB	*starts after the end of*	Late Iron I
64	Megiddo VA-IVB	*ends before the start of*	Iron IIB
65	Megiddo IVA	*starts after the end of*	Late Iron IIA
66	Megiddo H-12	*ends before the start of*	Late Iron I
67	Megiddo H-11	*ends before the start of*	Late Iron I
68	Megiddo H-10	*ends before the start of*	Late Iron I
69	Megiddo H-9	*ends before the start of*	Early Iron IIA
70	Megiddo H-8	*ends before the start of*	Late Iron IIA
71	Megiddo H-5	*starts after the end of*	Early Iron IIA
72	Megiddo H-5	*ends before the start of*	Iron IIB
73	Megiddo H-4	*starts after the end of*	Late Iron IIA
74	Megiddo H-3	*starts after the end of*	Late Iron IIA
75	Megiddo K-6	*ends before the start of*	Early Iron I
76	Megiddo K-5	*ends before the start of*	Late Iron I
77	Megiddo K-4	*ends before the start of*	Early Iron IIA
78	Megiddo K-2	*starts after the end of*	Early Iron IIA
79	Megiddo K-2	*ends before the start of*	Iron IIB
	Egyptian Synchronisms		
80	Megiddo VIIA	*ends after the start of*	Ramesses VI
81	Megiddo VIIA	*ends after the start of*	Ramesses III
82	Megiddo H-9	*ends after the start of*	Ramesses I
83	Megiddo K-8	*ends after the start of*	Amenhotep II
84	Megiddo K-8	*ends after the start of*	Ramesses I
85	Megiddo K-6	*ends after the start of*	Ramesses I
86	Megiddo K-9	*ends after the start of*	Amenhotep III
87	Megiddo H-15	*ends after the start of*	Ahmose I
88	Megiddo VIB	*ends after the start of*	Ramesses II
89	Megiddo VIA	*ends after the start of*	Ramesses I
90	Megiddo VIA	*ends after the start of*	Amenhotep III
91	Megiddo IVA	*ends after the start of*	Ramesses IV
92	Megiddo K-9	*ends after the start of*	Thutmose IV
	Bichrome Pottery		
93	Megiddo K-6	*ends before the start of*	Bichrome
94	Megiddo K-5	*is contemporaneous with*	Bichrome
95	Megiddo K-4	*is contemporaneous with*	Bichrome
96	Megiddo K-3	*starts after the end of*	Bichrome
97	Megiddo H-13	*ends before the start of*	Bichrome
98	Megiddo H-12	*is contemporaneous with*	Bichrome
99	Megiddo H-11	*is contemporaneous with*	Bichrome

No.	*Period 1*	*Synchronism*	*Period 2*
100	Megiddo H-10	*is contemporaneous with*	Bichrome
101	Megiddo H-9	*is contemporaneous with*	Bichrome
102	Megiddo H-8	*starts after the end of*	Bichrome
103	Megiddo VIIB	*ends before the start of*	Bichrome
104	Megiddo VIIA	*is contemporaneous with*	Bichrome
105	Megiddo VIB	*is contemporaneous with*	Bichrome
106	Megiddo VIA	*is contemporaneous with*	Bichrome
107	Megiddo VB	*starts after the end of*	Bichrome

Appendix B: Detailed Results of the Historical Model

Period	*Input Start*	*Input End*	*Input Duration*	*Computed Start*	*Computed End*	*Computed Duration*
			Strata			
IX	?	?	[50–150]	[−1643, −1217]	[−1493,−1167]	[50–150]
VIII	?	?	[50–150]	[−1493,−1167]	[−1343,−1117]	[50–150]
VIIB	?	?	[50–150]	[−1343,−1117]	[−1243,−1067]	[50–100]
VIIA	?	?	[50–100]	[−1243,−1067]	[−1143,−982]	[85–100]
Gap 1	?	?	[0–40]	[−1143,−982]	[−1143,−982]	[0–25]
VIB	?	?	[50–150]	[−1143,−982]	[−1093,−932]	[50–125]
VIA	?	?	[50–100]	[−1093,−932]	[−1043,−882]	[50–100]
Gap 2	?	?	[0–40]	[−1043,−882]	[−1043,−882]	[0–25]
VB	?	?	[50–100]	[−1043,−882]	[−993,−832]	[50–100]
VA-IVB	?	?	[50–150]	[−993,−832]	[−872,−782]	[50–150]
Gap 3	?	?	[0–40]	[−872,−782]	[−832,−782]	[0–40]
IVA	?	−732	[50–100]	[−832,−782]	−732	[50–100]
K-10	?	?	[50–150]	[−1643, -1217]	[−1493,−1167]	[50–150]
K-9	?	?	[50–150]	[−1493,−1167]	[−1343,−1117]	[50–150]
K-8	?	?	[50–100]	[−1343,−1117]	[−1243,−1067]	[50–100]
K-7	?	?	[10–50]	[−1243,−1067]	[−1233,−1057]	[10–25]
K-6	?	?	[50–100]	[−1233,−1057]	[−1183,−1007]	[50–65]
K-Gap 1	?	?	[0–40]	[−1183,−1007]	[−1183,−967]	[0–40]
K-5	?	?	[25–100]	[−1183,−967]	[−1143,−932]	[25–100]
K-4	?	?	[50–100]	[−1143,−932]	[−1043,−882]	[50–100]
K-Gap 2	?	?	[0–40]	[−1043,−882]	[−1043,−857]	[0–40]
K-3	?	?	[25–100]	[−1043,−857]	[−993,−832]	[25–100]
K-2	?	?	[50–150]	[−993,−832]	[−872,−782]	[50–150]
K-Gap 3	?	?	[0–40]	[−872,−782]	[−832,−782]	[0–40]
K-1	?	−732	[50–100]	[−832,−782]	−732	[50–100]
H-15	?	?	[50–150]	[−1643, 1207]	[−1493,−1157]	[50–150]
H-14	?	?	[50–150]	[−1493,−1157]	[−1343,−1107]	[50–150]
H-13	?	?	[50–150]	[−1343,−1107]	[−1233,−1057]	[50–125]
H-12	?	?	[50–100]	[−1233,−1057]	[−1183,−1007]	[50–65]
H-11	?	?	[25–100]	[−1183,−1007]	[−1143,−982]	[25–40]
H-10	?	?	[50–100]	[−1143,−982]	[−1093,−932]	[50–75]
H-9	?	?	[50–100]	[−1093,−932]	[−1043,−882]	[50–100]
H-Gap 1	?	?	[0–40]	[−1043,−882]	[−1043,−882]	[0–40]
H-8	?	?	[25–100]	[−1043,−882]	[−1018,−857]	[25–100]
H-7	?	?	[25–100]	[−1018,−857]	[−993,−832]	[25–100]
H-6	?	?	[25–100]	[−993,−832]	[−968,−807]	[25–100]
H-5	?	?	[25–100]	[−968,−807]	[−872,−782]	[25–100]
H-Gap 2	?	?	[0–40]	[−872,−782]	[−872,−767]	[0–40]

Period	*Input Start*	*Input End*	*Input Duration*	*Computed Start*	*Computed End*	*Computed Duration*
H-4	?	?	[10–50]	[−872,−767]	[−832,−757]	[10–50]
H-3	?	−732	[25–100]	[−832,−757]	−732	[25–100]
			Archaeological Periods			
LB I	?	?	[100–150]	[−1643, −1267]	[−1493,−1167]	[100–150]
LB IIA	?	?	[50–150]	[−1493,−1167]	[−1343,−1117]	[50–150]
LB IIB	?	?	[50–150]	[−1343,−1117]	[−1233,−1057]	[60–125]
LB III	?	?	[30–100]	[−1233,−1057]	[−1183,−1007]	[35–65]
Early Iron I	?	?	[50–100]	[−1183,−1007]	[−1093,−932]	[75–100]
Late Iron I	?	?	[50–100]	[−1093,−932]	[−1043,−882]	[50–100]
Early Iron IIA	?	?	[50–100]	[−1043,−882]	[−993,−832]	[50–100]
Late Iron IIA	?	?	[50–150]	[−993,−832]	[−872,−782]	[50–150]
Iron IIB	?	?	[50–100]	[−872,−782]	[−822,−682]	[50–100]
			Bichrome			
Bichrome	?	?	[50–200]	[−1183,−1007]	[−1093,−882]	[75–200]

Appendix C: Detailed Results of The Historical Model with Stratum VIIB Ending after Ramesses III's Accession

Period	*Input Start*	*Input End*	*Input Duration*	*Computed Start*	*Computed End*	*Computed Duration*
			Strata			
IX	?	?	[50–150]	[−1584, −1217]	[−1434,−1167]	[50–150]
VIII	?	?	[50–150]	[−1434,−1167]	[−1284,−1117]	[50–150]
VIIB	?	?	[50–150]	[−1284,−1117]	[−1184,−1067]	[50–100]
VIIA	?	?	[50–100]	[−1184,−1067]	[−1099,−982]	[85–100]
Gap 1	?	?	[0–40]	[−1099,−982]	[−1099,−982]	[0–40]
VIB	?	?	[50–150]	[−1099,−982]	[−1049,−932]	[50–125]
VIA	?	?	[50–100]	[−1049,−932]	[−999,−882]	[50–100]
Gap 2	?	?	[0–40]	[−999,−882]	[−999,−882]	[0–40]
VB	?	?	[50–100]	[−999,−882]	[−949,−832]	[50–100]
VA–IVB	?	?	[50–150]	[−949,−832]	[−872,−782]	[50–150]
Gap 3	?	?	[0–40]	[−872,−782]	[−832,−782]	[0–40]
IVA	?	−732	[50–100]	[−832,−782]	−732	[50–100]
K-10	?	?	[50–150]	[−1584, −1217]	[−1434,−1167]	[50–150]
K-9	?	?	[50–150]	[−1434,−1167]	[−1284,−1117]	[50–150]
K-8	?	?	[50–100]	[−1284,−1117]	[−1184,−1067]	[50–100]
K-7	?	?	[10–50]	[−1184,−1067]	[−1174,−1057]	[10–25]
K-6	?	?	[50–100]	[−1174,−1057]	[−1124,−1007]	[50–65]
K-Gap 1	?	?	[0–40]	[−1124,−1007]	[−1124,−967]	[0–40]
K-5	?	?	[25–100]	[−1124,−967]	[−1099,−932]	[25–100]
K-4	?	?	[50–100]	[−1099,−932]	[−999,−882]	[50–100]
K-Gap 2	?	?	[0–40]	[−999,−882]	[−999,−857]	[0–40]
K-3	?	?	[25–100]	[−999,−857]	[−949,−832]	[25–100]
K-2	?	?	[50–150]	[−949,−832]	[−872,−782]	[50–150]
K-Gap 3	?	?	[0–40]	[−872,−782]	[−832,−782]	[0–40]
K-1	?	−732	[50–100]	[−832,−782]	−732	[50–100]
H-15	?	?	[50–150]	[−1584, −1207]	[−1434,−1157]	[50–150]
H-14	?	?	[50–150]	[−1434,−1157]	[−1284,−1107]	[50–150]
H-13	?	?	[50–150]	[−1284,−1107]	[−1174,−1057]	[50–125]
H-12	?	?	[50–100]	[−1174,−1057]	[−1124,−1007]	[50–65]
H-11	?	?	[25–100]	[−1124,−1007]	[−1099,−982]	[25–40]

Period	*Input Start*	*Input End*	*Input Duration*	*Computed Start*	*Computed End*	*Computed Duration*
H-10	?	?	[50–100]	[−1099,−982]	[−1049,−932]	[50–75]
H-9	?	?	[50–100]	[−1049,−932]	[−999,−882]	[50–100]
H-Gap 1	?	?	[0–40]	[−999,−882]	[−999,−882]	[0–40]
H-8	?	?	[25–100]	[−999,−882]	[−974,−857]	[25–100]
H-7	?	?	[25–100]	[−974,−857]	[−949,−832]	[25–100]
H-6	?	?	[25–100]	[−949,−832]	[−924,−807]	[25–100]
H-5	?	?	[25–100]	[−924,−807]	[−872,−782]	[25–100]
H-Gap 2	?	?	[0–40]	[−872,−782]	[−872,−767]	[0–40]
H-4	?	?	[10–50]	[−872,−767]	[−832,−757]	[10–50]
H-3	?	−732	[25–100]	[−832,−757]	−732	[25–100]
Archaeological Periods						
LB I	?	?	[100–150]	[−1584, −1267]	[−1434,−1167]	[100–150]
LB IIA	?	?	[50–150]	[−1434,−1167]	[−1284,−1117]	[50–150]
LB IIB	?	?	[50–150]	[−1284,−1117]	[−1174,−1057]	[60–125]
LB III	?	?	[30–100]	[−1174,−1057]	[−1124,−1007]	[35–65]
Early Iron I	?	?	[50–100]	[−1124,−1007]	[−1049,−932]	[75–100]
Late Iron I	?	?	[50–100]	[−1049,−932]	[−999,−882]	[50–100]
Early Iron IIA	?	?	[50–100]	[−999,−882]	[−949,−832]	[50–100]
Late Iron IIA	?	?	[50–150]	[−949,−832]	[−872,−782]	[50–150]
Iron IIB	?	?	[50–100]	[−872,−782]	[−822,−682]	[50–100]
Bichrome						
Bichrome	?	?	[50–200]	[−1124,−1007]	[−1049,−882]	[75–200]

Appendix D: Detailed results of the Radiocarbon Model (68.2% Confidence Level)

Period	*Input Start*	*Input End*	*Input Duration*	*Computed Start*	*Computed End*	*Computed Duration*
Strata						
IX	?	?	[50–150]	[−1571, −1311]	[−1421,−1261]	[50–150]
VIII	?	?	[50–150]	[−1421,−1261]	[−1271,−1211]	[50–150]
VIIB	?	?	[50–150]	[−1271,−1211]	[−1171,−1161]	[50–100]
VIIA	?	?	[50–100]	[−1171,−1161]	[−1071,−1061]	[90–100]
Gap 1	?	?	[0–40]	[−1071,−1061]	[−1071,−1031]	[0–40]
VIB	?	?	[50–150]	[−1071,−1031]	[−1021,−981]	[50–90]
VIA	?	?	[50–100]	[−1021,−981]	[−971,−931]	[50–90]
Gap 2	?	?	[0–40]	[−971,−931]	[−971,−891]	[0–40]
VB	?	?	[50–100]	[−971,−891]	[−921,−832]	[50–100]
VA-IVB	?	?	[50–150]	[−921,−832]	[−871,−782]	[50–139]
Gap 3	?	?	[0–40]	[−871,−782]	[−832,−782]	[0–40]
IVA	?	−732	[50–100]	[−832,−782]	−732	[50–100]
K-10	?	?	[50–150]	[−1571, −1311]	[−1421,−1261]	[50–150]
K-9	?	?	[50–150]	[−1421,−1261]	[−1271,−1211]	[50–150]
K-8	?	[−1211, −1161]	[50–100]	[−1271,−1211]	[−1171,−1161]	[50–100]
K-7	?	[−1185, −1136]	[10–50]	[−1171,−1161]	[−1161,−1136]	[10–25]
K-6	?	[−1136, −1083]	[50–100]	[−1161,−1136]	[−1111,−1086]	[50–65]
K-Gap 1	?	?	[0–40]	[−1111,−1086]	[−1111,−1061]	[0–40]
K-5	?	?	[25–100]	[−1111,−1056]	[−1071,−1031]	[25–80]
K-4	?	?	[50–100]	[−1071,−1031]	[−971,−931]	[60–100]
K-Gap 2	?	?	[0–40]	[−971,−931]	[−971,−891]	[0–40]
K-3	?	?	[25–100]	[−971,−891]	[−921,−832]	[25–100]
K-2	?	?	[50–150]	[−921,−832]	[−871,−782]	[50–139]

Period	*Input Start*	*Input End*	*Input Duration*	*Computed Start*	*Computed End*	*Computed Duration*
K-Gap 3	?	?	[0–40]	[−871,−782]	[−832,−782]	[0–40]
K-1	?	−732	[50–100]	[−832,−782]	−732	[50–100]
H-15	?	?	[50–150]	[−1571, −1286]	[−1421,−1236]	[50–150]
H-14	?	?	[50–150]	[−1421,−1236]	[−1271,−1186]	[50–150]
H-13	?	[−1146, −1084]	[50–150]	[−1271,−1186]	[−1146,−1136]	[50–125]
H-12	?	[−1108, −1062]	[50–100]	[−1146,−1136]	[−1096,−1086]	[50–60]
H-11	?	[−1073, −1031]	[25–100]	[−1096,−1086]	[−1071,−1061]	[25–35]
H-10	?	[−1047, −1011]	[50–100]	[−1071,−1061]	[−1021,−1011]	[50–60]
H-9	?	?	[50–100]	[−1021,−1011]	[−971,−931]	[50–90]
H-Gap 1	?	?	[0–40]	[−971,−931]	[−971,−891]	[0–40]
H-8	?	?	[25–100]	[−971,−891]	[−946,−857]	[25–100]
H-7	?	?	[25–100]	[−946,−857]	[−921,−832]	[25–100]
H-6	?	?	[25–100]	[−921,−832]	[−896,−807]	[25–100]
H-5	?	?	[25–100]	[−896,−807]	[−871,−782]	[25–100]
H-Gap 2	?	?	[0–40]	[−871,−782]	[−871,−767]	[0–40]
H-4	?	?	[10–50]	[−871,−767]	[−832,−757]	[10–50]
H-3	?	−732	[25–100]	[−832,−757]	−732	[25–100]
Archaeological Periods						
LB I	?	?	[100–150]	[−1571, −1361]	[−1421,−1261]	[100–150]
LB IIA	?	?	[50–150]	[−1421,−1261]	[−1271,−1211]	[50–150]
LB IIB	?	?	[50–150]	[−1271,−1211]	[−1146,−1136]	[65–125]
LB III	?	?	[30–100]	[−1146,−1136]	[−1111,−1086]	[35–60]
Early Iron I	?	?	[50–100]	[−1111,−1086]	[−1021,−986]	[75–100]
Late Iron I	?	?	[50–100]	[−1021,−986]	[−971,−891]	[50–100]
Early Iron IIA	?	?	[50–100]	[−971,−891]	[−921,−832]	[50–100]
Late Iron IIA	?	?	[50–150]	[−921,−832]	[−871,−782]	[50–139]
Iron IIB	?	?	[50–100]	[−871,−782]	[−821,−682]	[50–100]
Bichrome						
Bichrome	?	?	[50–200]	[−1111,−1086]	[−1021,−891]	[75–200]

References

Asscher, Y., and Boaretto, E.
2019 "Absolute Time Ranges in the Plateau of the Late Bronze to Iron Age Transition and the Appearance of Bichrome Pottery in Canaan, Southern Levant." *Radiocarbon* 61.1: 13–37. https://doi.org/10.1017/RDC.2018.58

Asscher, Y., Cabanes, D., Hitchcock, L. A., Maeir, A. M., Weiner, S., and Boaretto, E.
2015 "Radiocarbon Dating Shows an Early Appearance of Philistine Material Culture in Tell es-Safi/Gath, Philistia." *Radiocarbon* 57.5: 1–26. https://doi.org/10.2458/azu_rc.57.18391

Asscher, Y., Lehmann, G., Rosen, S. A., Weiner, S., and Boaretto, E.
2015 "Absolute Dating of the Late Bronze to Iron Age Transition and the Appearance of Philistine Culture in Qubur el-Walaydah, Southern Levant." *Radiocarbon* 57.1: 77–97. https://doi.org/10.2458/azu_rc.57.16961

Ben-Dor Evian, S.
2017 "Ramesses III and the 'Sea-Peoples': Towards a New Philistine Paradigm." *Oxford Journal of Archaeology* 36.3: 267–85. https://doi.org/10.1111/ojoa.12115

Ben-Dor Evian, S., and Münger, S.
In press "Stamp-Seal Amulets." In I. Finkelstein and M. A. S. Martin (eds.), *Megiddo VI: The 2010–2014 Seasons*, 1300–24. Monograph Series of the Institute of Archaeology of Tel Aviv University. Tel Aviv: Emery and Claire Yass Publications in Archaeology.

Brandl, B.
2004 "Scarabs and Plaques Bearing Royal Names of the Early 20th Egyptian Dynasty Excavated in Canaan – from Sethnakht to Ramesses IV." In M. Bietak and E. Czerny (eds.), *Scarabs of the Second Millennium* BC *from Egypt, Nubia, Crete and the Levant: Chronological and Historical Implications. Papers of a Symposium, Vienna, 10th–13th January 2002*, 57–71. Contributions to the Chronology of the Eastern Mediterranean 8; Denkschriften der Gesamtakademie 35. Vienna: Austrian Academy of Sciences.

Breasted, J. H.
1948 "Bronze Base of a Statue of Ramesses VI Discovered at Megiddo." In G. Loud (ed.), *Megiddo II. Seasons of 1935–1939*, 135–38. Oriental Institute Publications 62. Chicago: University of Chicago.

Bronk Ramsey, C.
2009 "Bayesian Analysis of Radiocarbon Dates." *Radiocarbon* 51.1: 337–360. https://doi.org/10.1017/S0033822200033865

Buck, C. E., Kenworthy, J. B., Litton, C. D., and Smith, A. F. M.
1991 "Combining Archaeological and Radiocarbon Information: A Bayesian Approach to Calibration." *Antiquity* 65.249: 808–21. https://doi.org/10.1017/S0003598X00080534

Burke, A. A., Peilstöcker, M., Karoll, A., Pierce, G. A., Kowalski, K., Ben-Marzouk, N., Damm, J. C., Danielson, A. J., Fessler, H. D., Kaufman, B., Pierce, K. V. L., Höflmayer, F., Damiata, B. N., and Dee, M.
2017 "Excavations of the New Kingdom Fortress in Jaffa, 2011–2014: Traces of Resistance to Egyptian Rule in Canaan." *American Journal of Archaeology* 121.1: 85–133. https://doi.org/10.3764/aja.121.1.0085

Crema, E. R.
2012 "Modelling Temporal Uncertainty in Archaeological Analysis." *Journal of Archaeological Method and Theory* 19: 440–61. https://doi.org/10.1007/s10816-011-9122-3

Crema, E. R., and Kobayashi, K.
2020 "A Multi-proxy Inference of Jōmon Population Dynamics Using Bayesian Phase Models, Residential Data, and Summed Probability Distribution of ^{14}C Dates." *Journal of Archaeological Science* 117: 1–10. https://doi.org/10.1016/j.jas.2020.105136

Demján, P., and Dreslerová, D.
2016 "Modelling Distribution of Archaeological Settlement Evidence Based on Heterogeneous Spatial and Temporal Data." *Journal of Archaeological Science* 69: 100–9. https://doi.org/10.1016/j.jas.2016.04.003

Desachy, B.
2016 "From Observed Successions to Quantified Time: Formalizing the Basic Steps of Chronological Reasoning." *ACTA IMEKO* 5.2: 4–13. https://doi.org/10.21014/acta_imeko.v5i2.353

Falk, D. A.
2016 "Groundhog: A Computer Test Laboratory to Validate Chronological Hypotheses." Research poster presented at the 2016 Annual Meeting of the American Schools of Oriental Research (ASOR). http://www.groundhogchronology.com/poster.pdf
2020 "Computer Analytics in Chronology Testing and its Implications for the Date of the Exodus." In R. E. Averbeck and K. L. Younger Jr. (eds.), *"An Excellent Fortress for His Armies, a Refuge for the People," Egyptological, Archaeological, and Biblical Studies in Honor of James K. Hoffmeier*, 99–111. University Park, PA: Pennsylvania State University.

Finkelstein, I.
1995 "The Date of the Settlement of the Philistines in Canaan." *Tel Aviv* 22.2: 213–39. https://doi.org/10.1179/tav.1995.1995.2.213
1996 "Stratigraphy and Chronology of Megiddo and Beth-Shan in the 12th–11th Centuries B.C.E." *Tel Aviv* 23: 170–84. https://doi.org/10.1179/tav.1996.1996.2.170
2016 "To Date or Not to Date: Radiocarbon and the Arrival of the Philistines." *Egypt and the Levant* 26: 275–84. https://doi.org/10.1553/AEundL26s275

2018 "Philistine Chronology: An Update." *Israel Exploration Journal* 68.2: 221–31.

Finkelstein, I., and Piasetzky, E.
2010 "Radiocarbon Dating the Iron Age in the Levant: A Bayesian Model for Six Ceramic Phases and Six Transitions." *Antiquity* 84.324: 374–85. https://doi.org/10.1017/S0003598X00066643

Finkelstein I., Arie, E., Martin, M. A. S., and Piasetzky, E.
2017 "New Evidence on the Late Bronze/Iron I Transition at Megiddo: Implications for the End of the Egyptian Rule and the Appearance of Philistine Pottery." *Egypt and the Levant* 27: 261–80. https://doi.org/10.1553/AEundL27s261

Geeraerts, G., Levy, E., and Pluquet, F.
2017 "Models and Algorithms for Chronology." In S. Schewe, T. Schneider, and J. Wijsen (eds.), *Proceedings of the 24th International Symposium on Temporal Representation and Reasoning, TIME 2017, October 16–18, 2017, Mons, Belgium*, 13:1–13:18. Leibniz International Proceedings in Informatics 90. Saarbrücken/Wadern: Schloss Dagstuhl – Leibniz-Zentrum für Informatik. https://doi.org/10.4230/LIPIcs.TIME.2017.13

Harrison, T. P., ed.
2004 *Megiddo 3, Final Report on the Stratum VI Excavations*. Oriental Institute Publications 127. Chicago: The Oriental Institute.

Holst, M. K.
2004 "Complicated Relations and Blind Dating: Formal Analysis of Relative Chronological Structures." In C. E. Buck and A. R. Millard (eds.), *Tools for Constructing Chronologies: Crossing Disciplinary Boundaries*, 129–47. London: Springer. https://doi.org/10.1007/978-1-4471-0231-1_6

Johnson, I.
2004 "Aoristic Analysis: Seeds of a New Approach to Mapping Archaeological Distributions Through Time." In K. Fischer-Ausserer, W. Börner, M. Goriany, and L. Karlhuber-Vöckl (eds.), *Enter the Past. The E-Way into the Four Dimensions of Cultural Heritage. CAA2003, Computer Applications and Quantitative Methods in Archaeology*, 448–52. BAR International Series 1227. Oxford: Archaeopress.

Kahn, D.
2011 "The Campaign of Ramesses III Against Philistia." *Journal of Ancient Egyptian Interconnections* 3.4: 1–11.

Keel, O.
2013 "Stamp-seal Amulets." In I. Finkelstein, D. Ussishkin, and E. H. Cline (eds.), *Megiddo V: The 2004–2008 Seasons*, 977–92. Monograph Series of the Institute of Archaeology of Tel Aviv University 31. Tel Aviv: Emery and Claire Yass Publications in Archaeology, Institute of Archaeology, Tel Aviv University.

Kempinski, A.
1989 *Megiddo. A City State and Royal Centre in North Israel*. Materialien zur Allgemeinen und Vergleichenden Archäologie 40. Munich: Beck.

Kitchen, K. A.
2000 "Regnal and Genealogical Data of Ancient Egypt (Absolute Chronology I). The Historical Chronology of Ancient Egypt: A Current Assessment." In M. Bietak (ed.), *The Synchronisation of Civilisations in the Eastern Mediterranean in the Second Millennium B.C. Proceedings of an International Symposium at Schloß Haindorf (November 15–17, 1996) and at the Austrian Academy (Vienna, May 11–12, 1998)*, 39–52. Contributions to the Chronology of the Eastern Mediterranean I. Vienna: Austrian Academy of Sciences.

Kromholz, A. H.
1987 "Business and Industry in Archaeology." In: P. Ahström (ed.), *High, Middle or Low? (Part 1). Acts on an International Colloquium on Absolute Chronology Held at the University of Gothenburg, 20th–22nd August 1987*, 119–137. Gothenburg: Paul Ahströms Förlag.

Lamon, R. S., and Shipton, G. M.
1939 *Megiddo I: Seasons of 1925–1934, Strata I–V*. Oriental Institute Publications 42. Chicago: The Oriental Institute.

Levy, E., Geeraerts, G., Pluquet, F., Piasetzky, E., and Fantalkin, A.
2021 "Chronological Networks in Archaeology: A Formalised Scheme." *Journal of Archaeological Science* 127: 1–27. https://doi.org/10.1016/j.jas.2020.105225

Levy, E., Piasetzky, E. and Fantalkin, A.
2021 "Archaeological Cross-Dating: A Formalized Scheme." *Archaeological and Anthropological Sciences* 13: 1–30. https://doi.org/10.1007/s12520-021-01371-8

Levy, E., Piasetzky, E., and Finkelstein, I.
2020 "Strata, Scarabs and Synchronisms: A Framework for Synchronizing Strata and Artifacts." *Journal of Computer Applications in Archaeology* 3.1: 1–17. https://doi.org/10.5334/jcaa.41

Loud, G.
1939 *The Megiddo Ivories*. Oriental Institute Publications 52. Chicago: The University of Chicago.
1948 *Megiddo II. Seasons of 1935–1939*. Oriental Institute Publications 62. Chicago: The University of Chicago.

Martin, M. A. S.
2017a "The Fate of Megiddo at the End of the Late Bronze IIB." In O. Lipschits, Y. Gadot, and M. J. Adams (eds.), *Rethinking Israel, Studies in the History and Archaeology of Ancient Israel in Honor of Israel Finkelstein*, 267–86. Winona Lake, IN: Eisenbrauns.
2017b "The Provenance of Philistine Pottery in Northern Canaan, with a Focus on the Jezreel Valley." *Tel Aviv* 44.2: 193–231. https://doi.org/10.1080/03344355.2017.1357310

Porter, B., and Moss, R.
1952 *Topographical Bibliography of Ancient Egyptian Hieroglyphic Texts, Statues, Reliefs and Paintings,* Vol. VII, *Nubia, the Deserts and Outside Egypt*. Oxford: Griffith Institute, Ashmolean Museum.

Schneider, T.
2010 "Contributions to the Chronology of the New Kingdom and the Third Intermediate Period." *Egypt and the Levant* 20: 373–403. https://doi.org/10.1553/AEundL20s373

Ussishkin, D.
1985 "Levels VII and VI at Tel Lachish and the End of the Late Bronze Age in Canaan." In J. N. Tubb (ed.), *Palestine in the Bronze and Iron Ages, Papers in Honour of Olga Tufnell*, 213–28. Occasional Publication 11. London: Institute of Archaeology, University of London.
1995 "The Destruction of Megiddo at the End of the Late Bronze Age and its Historical Significance." *Tel Aviv* 22.2: 240–67. https://doi.org/10.1179/tav.1995.1995.2.240
2018 *Megiddo-Armageddon. The Story of the Canaanite and Israelite City*. Jerusalem: Israel Exploration Society, Biblical Archaeology Society.